Intra-specific variation and allometry of the skull of Late Cretaceous side-necked turtle *Bauruemys elegans* (Pleurodira, Podocnemididae) and how to deal with morphometric data in fossil vertebrates

Thiago F. Mariani Corresp., [1] , **Pedro S. R. Romano** [1]

[1] Deparatamento de Biologia Animal, Universidade Federal de Viçosa, Viçosa, MG, Brazil

Corresponding Author: Thiago F. Mariani
Email address: tmariani.bio@gmail.com

Background. Previous quantitative studies on *Bauruemys elegans* (Suárez, 1969) shell variation, as well as the taphonomic interpretation of its type locality, have suggested that all specimens collected in this locality may have belonged to the same population. We rely on this hypothesis in a morphometric study of the skull. Also, we tentatively assessed the eating preference habits differentiation that might be explained as due to ontogenetic changes. **Methods.** We carried out an ANOVA testing 29 linear measurements from 21 skulls of *B. elegans* taken by using a caliper and through images, using the ImageJ software. A Principal Components Analysis (PCA) was performed with 27 measurements (excluding total length and width characters; =raw data) in order to visualize the scatter plots based on the form variance only. Then, a PCA was carried out using ratios of length and width of each original measurement to assess shape variation among individuals. Finally, original measurements were log-transformed to describe allometries over ontogeny. **Results.** No statistical differences were found between caliper and ImageJ measurements. The first three PCs of the PCA with raw data comprised 70.2% of the variance. PC1 was related to size variation and all others related to shape variation. Two specimens plotted outside the 95% ellipse in PC1~PC2 axes. The first three PCs of the PCA with ratios comprised 64% of the variance. When considering PC1~PC2, all specimens plotted inside the 95% ellipse. In allometric analysis, five measurements were positively allometric, 19 were negatively allometric and three represent truly negative allometry. Many bones of the posterior and the lateral emarginations lengthen due to increasing size, while jugal and the quadratojugal decrease in width. **Discussion.** ImageJ is useful in replacing caliper since there was no statistical differences. Yet, iterative imputation is more appropriate to deal with missing data in PCA. Some specimens show small differences in form and shape. Form differences were interpreted as occuring due to ontogeny, whereas shape differences are related to feeding changes during growth.

Moreover, all outlier specimens are crushed and/or distorted, thus the form/shape differences may be partially due to taphonomy. The allometric lengthening of the parietal, quadrate, squamosal, maxilla, associated with the narrowing of jugal and quadratojugal may be related to changes in feeding habit between different stages of development. This change in shape might represent a progressive skull stretching and enlargement of posterior and lateral emargination during ontogeny, and consequently, the increment of the feeding-apparatus musculature. Smaller individuals may have fed on softer diet, whereas larger ones probably have had a harder diet, as seen in some living species of *Podocnemis*. We conclude that the skull variation might be related to differences in feeding habits over ontogeny in *B. elegans*.

Intra-specific variation and allometry of the skull of Late Cretaceous side-necked turtle *Bauruemys elegans* (Pleurodira, Podocnemididae) and how to deal with morphometric data in fossil vertebrates

Thiago Fiorillo Mariani[1], Pedro Seyferth R. Romano[1]

[1] Departamento de Biologia Animal, Universidade Federal de Viçosa, Viçosa, Minas Gerais, Brazil.

Corresponding author:

Thiago Mariani[1]

Av. P. H. Rolfs, Anexo do Centro de Ciências Biológicas II, Third Floor, Room 305, Viçosa, Minas Gerais, 36570-900, Brazil

Email address: tmariani.bio@gmail.com

19

20

21 **1. Introduction**

22 **1.1. Principal Component Analysis and fossil sampling bias**

23 Paleontological data are intrinsically scarce (Strauss, Atanassov & Oliveira, 2003; Hammer &
24 Harper, 2006), leading to incomplete data sampling. This limitation impacts several approaches
25 in paleontological studies, especially inter-specific variation analyses. Although there are some
26 methodologiesproposed to deal with missing entries in fossil quantitative datasets (e.g. Norell &
27 Wheeler, 2003; Strauss, Atanassov & Oliveira, 2003), sometimes the study relies on an
28 exploratory evaluation of general structure and Principal Component Analysis (PCA) is
29 commonly used for this purpose.

30 PCA is a method to ordinate multivariate data. Its aim is to identify the variables that account for
31 the majority of the variance within a multivariate matrix, by means of linear combinations of all
32 variables, which are converted into components that are independent of each other (Strauss,
33 Atanassov & Oliveira, 2003; Hammer, Harper & Ryan, 2001). Hence, PCA summarizes a large
34 amount of the variance contained in the data (Krzanowski,1979; Hammer, Harper & Ryan,
35 2001). It thus reduces a multidimensional space into fewer components which retain the majority
36 of the variance of a given sample (Jolicoeur & Mosimann, 1960; Peres-Neto, Jackson & Somers,
37 2003), and is therefore an useful tool for exploring large, complex data sets, being largely
38 applied to both extant and turtles (e.g. Jolicoeur & Mosimann, 1960; Claude et al., 2004;
39 Depecker et al., 2005, 2006; Werneburg et al., 2014; Ferreira et al., 2015).

40 **1.2. Case-study**

41 **1.2.1. Skull variation**

42 The skull is one of the most variable structures in vertebrates because it concentrates several
43 sensory organs, the brain, and the beginning of the respiratory and digestory systems, including
44 chewing muscles (Smith, 1993). Consequently, the skull is the body partwith more phenotypes
45 used in vertebrate cladistic analysis (Rieppel, 1993), as seen in turtles, in which most cladistic
46 analysis rely mainly on cranial characters (e.g. Gaffney et al., 1991; de la Fuente, 2003; Gaffney
47 et al., 2006, 2011; Joyce, 2007; Joyce & Lyson, 2010; Sterli et al., 2010; Sterli & de la Fuente,
48 2011a, b; Anquetin, 2012; Rabi et al., 2013; Romano et al., 2014; Ferreira et al., 2015; Romano,
49 in press). Despite that, most skull materials found in paleontological record of turtles are rare
50 and/or damaged due to the fossilization process bias, not allowing intraspecific comparisons or
51 ontogenetic inferences on most fossil turtle species known. Some exceptions are found in
52 Sanchéz Villagra & Winkler (2006) and Ferreira et al. (2016), who performed interspecific
53 comparisons among fossil turtle taxa using skull material..

54 **1.2.2. *Bauruemys* taxonomy**

55 *Bauruemys elegans* (Suárez, 1969) is a Late Cretaceous freshwater side-necked turtle found at
56 the Pirapozinho site (Suárez, 2002), in western São Paulo state. This species was originally
57 described as *Podocnemis* in three different communications by Suárez (1969a, b, c) and such
58 recognition was based on the overall similarities of the skull and shell to this living genus, a
59 common practice that time. Other South American Cretaceous side-necked turtles were initially
60 identified as *Podocnemis* as well, such as the *nomina dubia "Roxochelys" harrisi* (Pacheco,
61 1913) and *"Bauruemys" brasiliensis* (Staeche, 1937) and the *incertae sedis "Podocnemis"*

argentinensis (Cattoi & Freiberg, 1958) (see Romano et al., 2013 for a revision on Bauru Group species). Kischlat (1994) was the first to point out that all *Podocnemis* reported from the Cretaceous were doubtful and proposed a new genus, *Bauruemys*, to include *B. elegans* and, tentatively, *B. brasiliensis.* His conclusion was based on similarities of the plastron of both species, besides the analysis of cranial features in *B. elegans.* More recently, Romano et al. (2013) confirmed the recognition of *B. brasiliensis* as *Bauruemys,* but considering this species as *nomem dubium.* Kischlat (1994) and Kischlat et al. (1994) also pointed out that *B. elegans* could belong to Podocnemididae, but they did not test their hypothesis. Romano & Azevedo (2006) were the first to carry out a cladistic analysis to access the phylogenetic position of *Bauruemys*, placing it as a stem-Podocnemididae, i.e.: the sister group of all other Podocnemididae, which was consistently confirmed by subsequent analyses with more podocnemidid species included as terminals (França & Langer, 2006; Gaffney et al., 2011; Oliveira, 2011; Cadena, Bloch & Jaramillo, 2012).

1.2.3. Geological settings and taphonomic context of the Tartaruguito site

The Pirapozinho site, long ago known as "Tartaruguito" and formally assigned as such by Romano & Azevedo (2007) and Gaffney et al. (2011), is an Upper Cretaceous outcrop from the Presidente Prudente Formation, Bauru Basin (Geology *sensu* Fernandes & Coimbra, 2000). It is located in Pirapozinho municipality, São Paulo State, Brazil (Fig. 1). The "Tartaruguito" name, which means "turtle in rock" (*tartaruga*, from Portuguese, turtle; *ito*, from Latin, rock), reflects the great amount of turtle specimens found at that place. It is comparable to other rich fossil turtle localities, such as (1) the recently discovered Middle Jurassic Qigu Formation of the Turpan Basin in China (Wings et al., 2012; Rabi et al., 2013); (2) the Late Cretaceous (Maastrichtian) Hell Creek Formation ('Turtle Graveyard') in Slope County, North Dakota, USA

(Lyson & Joyce, 2009); (3) the Middle-Upper Paleocene Cerrejón Formation in Colombia (Jaramillo et al., 2007; Cadena et al., 2010; Cadena, Bloch & Jaramillo, 2012; Cadena et al., 2012); and (4) the Upper Miocene Urumaco Formation ('Capa de tortugas') in Venezuela (Aguilera, 2004; Sánchez-Villagra & Aguilera, 2006; Sánchez-Villagra & Winkler, 2006; Riff et al., 2010; de la Fuente, Sterli & Maniel, 2014). The two latter localities are near-shore marine coastal deposits with influence of freshwater rivers (Jaramillo et al., 2007; Gaffney et al., 2008), whereas the two former and the Tartaruguito site correspond to sediments that had been deposited in a riverine system with seasonal droughts in which turtles gathered in retreating, ephemeral water pools and died when habitat dried up completely (Soares et al., 1980; Fulfaro and Perinotto, 1996; Fernandes & Coimbra, 2000; Henriques et al., 2002, 2005; Suárez, 2002; Murphy et al., 2003; Bertini et al., 2006; Henriques, 2006; Wings et al., 2012). The Tartaruguito is also the type-locality of the peirosauridcrocodile *Pepesuchus deiseae* Campos, Oliveira, Figueiredo, Riff, Azevedo, Carvalho & Kellner, 2011 (Campos et al., 2011).

The general lithology of the Tartaruguito site is composed of cyclic alternations of sandstones and mudstones deposited in a meandering fluvial system with crevasse splays (Fernandes & Coimbra, 2000; Henriques et al., 2005; Bertini et al., 2006). Many articulated and complete fossils are found in these sequences, which indicate seasonal low energy floods (mudstones) followed by droughts (sandstones) in the region during the Late Cretaceous (Henriques et al., 2002, 2005; Henriques, 2006). Because only medium- to large-sized fossil specimens are found at the locality, it is assumed that the Tartaruguito site was a foraging area for turtles (D. Henriques, pers. comm.). Thus, the fossil assemblage probably represents several episodes of floods and droughts. The flood periods might have allowed foraging areas expansion for turtles

and crocodiles, while during the dry seasons turtles gathered on the remnants of water pools and some died when pools dried up completely (Henriques et al., 2002, 2005; Henriques, 2006).

That being said, we consider that all turtle specimens found at the Tartaruguito site might correspond to subadults to adult ages, and it is reasonable to assume that all *B. elegans* individuals collected in the Tartaruguito site might have belonged to a single population (agreeing with Henriques et al., 2002, 2005; Henriques, 2006; Romano & Azevedo, 2007). Indeed, as suggested by Romano & Azevedo (2007), this single population would consist on different generations of turtles' corpses grouped in the same locality. One might consider that size differences might be due to sexual dimorphism (R. Hirayama and S. Thomson, pers. comm.), in which the females would be larger and have more posteriorly extended carapaces than the males. However, sexual dimorphism on podocnemidid turtles can be assessed only on shell shape and our data is based mostly on isolated skulls (see Material and Methods). As a consequence, although it is possible that sexual dimorphism may affect measurements captured in this study, we did not consider it, given the lack of evidence to assume such outcome. Also, to our knowledge, skull shape differences related to sexual dimorphism has never been described to podocnemidid turtles yet. Moreover, Romano & Azevedo (2007) were not able to reject the single population hypothesis using shell measurements (from both plastron and carapace) in a morphometric approach neither to describe sexual dimorphism in the data, concluding that the differences were due to ontogenetic variation. Therefore, we highlight that we are assuming the population definition of Futuyma (1993), as taken on by Romano & Azevedo (2007), that a population is a conjunct of semaforonts temporally connected, i.e., a sequence of individuals from different generations, and limited in a restricted space, in this case, the Tartaruguito site. By

129 assuming this, we explicitly follow Hennig's (1966) semaphoront concept, on which a species is
130 modifiable (i.e. not strictly typological) and represented by a sequence of generations.

131 **1.3. Objectives**

132 Efforts to study fossil materials may be hampered by difficulty in accessing foreign collections.
133 It can narrow and even preclude their studies. In addition, given the missing data problem
134 inherent to fossil record, the way one treatsthe missing entries in morphometric studies can affect
135 the results and conclusions. Regarding the use of caliper or ImageJ in taking measurements, here
136 we tested both approaches by taking linear measurements for morphometric studies based on
137 photographs (e.g. Bailey, 2004) and also evaluated how different approaches designed to deal
138 with missing data can impact results of exploratory statistical procedures and data interpretation
139 by comparing two different substitution algorithms of missing entries. These procedures are
140 exemplified using a real paleontological data set and with paleobiological inferences.
141 Considering the case-study, we explored the variation in skulls among individuals of *Bauruemys*
142 *elgans* from different ages and generations. and described the differences in skull morphology
143 along the ontogeny of the species and discuss the probable consequences of such variation to the
144 diet preferences changes along the growth.

145 **2. Material and Methods**

146 **2.1. Sample and characters**

147 Twenty-one skulls of *Bauruemys elegans* were examined in this study, including the type series
148 plus nineteen topotypes: AMNH-7888, LPRP0200, LPRP0369, LPRP0370, MCT 1492-R
149 (holotype), MCT 1753-R (paratype), MCZ 4123, MN 4322-V, MN 4324-V, MN 6750-V, MN
150 6783-V, MN 6786-V, MN 6787-V, MN 6808-V, MN 7017-V, MN 7071-V, MZSP-PV29,

MZSP-PV30, MZSP-PV32, MZSP-PV34, and MZSP-PV35. We established 39 landmarks (Fig. 2) that decompose the overall shape of the skull in order to take measurements between two landmarks. Since most of the specimens have deformation and breakage, we could not perform a geometric morphometric analysis using the landmarks because the taphonomical bias would incorporate error to the analysis of form and shape. Thus, we used the landmarks to set up 29 traditional morphometric characters that correspond to a linear measurement between two landmarks (all characters are described in table 1). Also, the use of landmarks to set up the measurements is useful to maintain the same anatomic references for all characters in each specimen, since the landmarks enable a better description of morphological variation and establishment of linear measurements, as performed by Romano & Azevedo (2007) with shell morphometric characters. All measurements were taken on the same side of the skull (right side) unless the characters could not be measured due to deformation or breakage. We are aware that deeper structures (z-axis) can influence the straight line between two landmarks in 2D images and used ImageJ version 1.47 (Rasband, 1997) to take the measurements after comparing its accuracy with the caliper (Mariani & Romano, 2014). This procedure was necessary because we obtained photos of skulls in dorsal, ventral, and lateral views housed in foreign collections and did not perform the described measurements (see table 1) using caliper in such specimens because they were analyzed prior to this study. The error test between measurements taken using caliper and ImageJ using part of the sample are described below. We followed the bone nomenclature of Parsons & Williams (1961) and extended by Gaffney (1972, 1979) (see all abbreviations after Conclusion topic).

2.2. Statistical analyses

2.2.1. Preliminary analysis: Caliper vs. ImageJ

Before carrying out others statistical analyses, we compared the same characters data set (Data S1) of a sub-sample by using two different approaches (= treatments): measurements taken using caliper and measurements taken using photographs via ImageJ. This comparison was necessary in order to evaluate whether or not the two measurements methods are significantly different. Then, we performed an One-way Analysis of Variance (ANOVA) comparing the 29 measurements in 12 specimens (LPRP0200, LPRP0369, LPRP0370, MN4322-V MN4324-V, MN6750-V, MN6783-V, MN6786-V, MN6787-V, MN6808-V, MN7017-V, and MN7071-V). Two groups of variables were established: measurements taken directly from specimens using caliper (preliminary data set 1) and the same characters taken from photographs of the same specimens using ImageJ (preliminary data set 2). All characters taken using photographs/ImageJ that did not show significant differences to their correspondents taken by caliper were used on the subsequent statistical analyses of form and shape differences among the sample of *Bauruemys elegans*. By doing that, the sample was increased without including error and incomparable characters (i.e.: by using different measurement techniques).

We found most of the measurements do not differ statistically ($p>0.05$) between the two treatments (caliper and ImageJ; table 1). However, one measurement, length of maxilla (LMX), had statistical difference ($p=0.017$) between the treatments, because the maxilla is a curved structure and thus the landmarksare in different positions (LM 24 is deeper and farther from the camera in relation to LM11) in relation to the plane the picture was taken. Given that no statistical differences were found in almost all characters, ImageJ could be an economic and time-saving tool for morphometric analyses from photographs (2D), and could be applied by scientists at distant institutions.

196 The study *in situ* of the material is preferable, although pictures are an economic alternative in
197 where cases one is not able to handle the material. We must aware that one have to choose one of
198 the two treatments to construct a morphometric matrix, otherwise it will be composed of values
199 obtained by two diffent methods.

200 **2.2.2. Univariate, multivariate and allometric analyses**

201 Three analyses using the complete sample were carried out: (1) a descriptive statistics (mean,
202 standard deviation, median, variance, maximum and minimum values) of all characters (Data
203 S2), (2) an allometric analysis of length and width characters correlating them to total length and
204 width measurements (Data S3), and (3) a multivariate non-parametric exploratory statistics via
205 Principal Component Analysis (PCA). The latter was divided into two different PCAs: (3.1)
206 using 27 characters from the raw data matrix (total length and width characters were excluded in
207 this analysis; Data S4 – because PCA is sensitive to wide-scale variations in the original
208 measurements), and (3.2) using 27 charactersthat correspond to the proportions of each character
209 from the raw data (i.e. original measurements) represented by its length or width characters
210 divided by each individual total length or width (e.g. the length of MCZ4312 postorbital divided
211 by the total length of the skull of this specimen; see complete data in Data S5). All statistical
212 analyses were performed using the software PAST version 3.05 (Hammer et al., 2001).

213 In the allometric analysis (analysis 2, Data S3), all characters were previously log-transformed
214 and a linear regression was carried out separately for length and width characters, using the least
215 square fitting approach for residuals. We established the allometries by considering the
216 regression's slope, i.e. the coefficient a, as following: positive allometry ($a>1$), negative
217 allometry ($1>a>0$), enantiometry ($a<0$), and isometry ($a=1$).

In the first PCA approach (3.1) we excluded total length and width characters because of their high influence on the PCA result, since higher values compose the majority of the summarized variance in PC's (Mingoti, 2013), and because of the redundancybetween these measurements and the others. We also assessed differences by applying two different substitution algorithms for missing data in PAST, using the default "mean value imputation" option (i.e. missing data are replaced by the column average), and the alternative "iterative imputation" option, which computes a regression upon an initial PCA until it converges to missing data estimations, replacing missing data by such estimations (Ilin & Raiko, 2010). The latter is recommended and, after comparing both results, we selected it (see supplemental material 3 to visualize PCA results computed using PAST's default option approach). The second PCA (3.2) was conducted to remove the effect of size (=growth) and perform an exploratory analysis of the shape alone. Six specimens were removed from this analysis because they were broken and the total length or width measures were not measurable.

The univariate analysis was made in order to quantify and describe the variation of the characters set in *Bauruemys elegans* skull, using the assumption thatthe sample is representative of a single population. The linear regression analyses allowed us to make inferences about osteological shape change related to size change, i.e., related to growth, by assuming that bigger specimens are older than smaller ones. This approach is, therefore, a study of allometry (*sensu* Huxley & Teissier, 1936; Huxley, 1950; Gould, 1966; Gould, 1979; Somers, 1989; Futuyma, 1993) and the assumption of correlation between size and aging is based on continuous growth to be common on extant turtles (Klinger & Musick, 1995; Shine & Iverson, 1995; Congdon et al., 2003). Since the use of a parametric statistic was infeasible due to the nature of the sample (i.e.: a small datasetthat do not show homoscedasticity and normality), the PCAs were used to search for a

structure of the data that matches to the pattern found by Romano & Azevedo (2007) using shell characters (i.e. all individuals plotted inside the 95% confidence ellipse). If the pattern observed is similar to previous morphometric and taphonomic inferences, then the variation is not enough to assume that the sample represents different populations of *Bauruemys elegans* or a different species (see section 4.1.2). In other words, since a parametric test is not feasible with statistical confidence, the lack of structure in the PC plots were herein interpreted as a fail to the attempt of falsifying the single population hypothesis. All principal components were, therefore, analyzed but we present only those with higher variance.

3. Results

3.1. Descriptive Analysis

The results of the descriptive statistics are summarized in table 2. As expected, values of total length and width (TLS and WLS) were the most variable among all measurements, because the variation scale in these characters is greater than in others measurements. Characters of the bones forming the upper temporal fossa (i.e. PA, QJ, SQ, QU and OP) had great variation, with the parietal being the most variable in length (SD=6.45) and the least variable in width (SD=2.94), whereas quadratojugal obtained the smallest variation in length (SD=2.38) and the greatest in width (SD=4.03). Among the characters of the bones forming the lower temporal fossa (i.e. JU, MX, PO, PT and PAL), the variation in length was in general greater than in width. Postorbital and maxilla had almost the same variation in length (SD=4.12 and SD=4.11, respectively); WPO had the smallest variation within the group of bones forming the lower temporal fossa (SD=1.83); and the stretch of the maxilla had the greatest variation (SD=7.63) of all characters measured. Characters of the other bones had smaller values than the aforementioned bones, with

the exception of WPO which was smaller than LFR (SD=2.08), LVO (SD=1.95), LBO (SD=2.12),WFR (SD=1.88) and WBS (SD=2.19).

3.2. Allometric Analysis

Among all comprised measurements, three were truly negatively allometric (LPF, WJU and WQJ); five were positively allometric (LPAL, LPT, LPO, WPF and WPO); and the others were negatively allometric. It is also worth to note that two were not isometric [WPF (a=1,0074; p=0.0009) and WOP (a=0.98159; p=0.007)], although presented angular coefficient very close to 1. All regressions are shown in figures 3, 4 and 5.

3.3. Principal Component Analysis (PCA)

3.3.1. Raw data

3.3.1.1. Replacing missing data with mean values

By using the "mean value imputation" approach, a total of 70.32% of the variance was comprised by the first three principal components (PC1=42.15%; PC2=16.82%; PC3=11.35%), so that the others were less significant for the analysis by following the broken stick model, and are not presented. We interpreted that PC1 variation is due to size variation because an approach using all characters has shown a similar plot (see Fig. 6A). PC2 and PC3 seems to represent shape differences between individuals. In all PC individual projections (Fig. 6A and 6B) most of specimens were included inside the 95% confidence ellipse. Two exceptions are MCZ4123 and MN7071-V, which have not been included in the ellipse when PC1 vs. PC2 were considered (Fig. 6A); also the former was outside the ellipse in PC2 vs. PC3 scatter plot (Fig. 6B),

indicating shape differences of these specimens. However, both specimens have suffered different degrees of crushing due to taphonomic bias and that is likely the reason for this result.

In PC1' loadings (Table 3), only two characters were negatively related (LPF and WJU); SMX, LPA and LPO loadings were the highest related (L=0.69; L=0.27; L=0.36, respectively); and the rest of characters obtained intermediate values [e.g. LPT (L=0.17), LMX (L=0.18), WOP (L=0.21)]. PC2 has shown a high relation with character LPA (L=0.77), showing possible changes in shape in this region, and a negative loading for SMX (L= -0.38), whereas the others had no significant scores. The last considered principal component (=PC3), showed high correlations with bones in both lateral and posterior emarginations of the skull [LMX (L=0.68), WMX (L=0.25), LJU (L=0.30), WQJ (L=0.29) and LQU (L=0.32)] and, as the results in PC2, allows inferences in shape changes of these regions.

3.3.1.2. Replacing missing data with regression estimation

The alternative missing data approach (i.e. "iterative imputation"; Fig. 6C) generated two principal components which comprised 88.96% of the total variance (PC1=53.01%; PC2=35.95%). In contrast with the previous approach, PC1 was interpreted as representing shape and PC2 reflected size variations. In addition, all specimens were included inside the 95% ellipse in PC1vs.PC2 scatter plot. The specimen MN7017-V, interestingly, was excluded from the ellipse when considering PC2 vs. PC3, but the percentage of variance represented by PC3 is too low (PC3=3.28%) to assume any difference from the others individuals. We agree with Ilin & Raiko (2010) and prefer to choose the iterative imputation approach for dealing with missing entries (see discussion on session 4.1). Then, discussions concerning the form variation in our data are related to PCA analysis using iterative imputation.

In PC1 loadings (Table 3), LPA, WPA and LSQ were the highest positively related characters (L=0.89; L=0.22; L=0.16, respectively), whereas LMX, LJU, LQJ, WQJ and LQU were the highest negatively related characters (L= -0.18; L= -0.14; L= -0.16; L= -0.11; L= -0.11; L= -0.13, respectively). Only two characters were negative for PC2 (LPF and WJU), whereas the rest of the coefficients were positive. Among them, SMX was the highest (L=0.59); WPAL, WBS, LBO, LJU, LQU, LPO and WOP obtained intermediate scores (L=0.23; L=0.19; L=0.20; L=0.19; L=0.21; L=0.29; L=0.30, respectively); the others were less related [e.g. LPA (L=0.04), LPT (L=0.13) and WPO (L=0.10)]. In general, the values indicate that in *B. elegans* most changes occur in bones of both lateral and temporal emargination.

3.3.2. Shape characters (proportions)

3.3.2.1. Replacing missing data with mean values

When applying "mean value imputation", 53.99% of the variance were comprised by the first two principal components (PC1=35.29%; PC2=18.70%), both corresponding to shape, as all units of measurements were removed through the division of characters before carrying out the analysis. All specimens were comprised into the 95% confidence ellipse (Fig. 7A).

The first PC was positively related to the loadings values of LPA/TLS (L=0.28), LMX/TLS (L=0.38), LQU/TLS (L=0.27), WPA/TWS (L=0.23), SMX/TWS (L=0.38), WMX/WTS (L=0.35), WQJ/TWS (L=0.48); the most negative values were LPO/TLS (L= -0.16) and WOP/TWS (L= -0.13). The second PC was positively related to LPA/TLS (L=0.66), WPA/TWS (L=0.32)WOP/TWS (L=0.27), and negatively to LMX/TLS (L= -0.50) (see Table 4 for all loading values). It is interesting to note that most of highly-related proportions were in reference

to bones associated either with feeding *apparatus* (squamosal, parietal, quadratojugal and jugal) or catching food and trituration surface (maxilla).

3.3.2.2. Replacing missing data with regression estimation

The "iterative imputation" substitution model of missing data explained 77.35% of the variance comprised by two principal components (PC1=45.49%; PC2=31.86), both representing shape. All specimens were included in the confidence ellipse (Fig. 7B), thus shape differences do not indicate possible different populations or species.

PC1 was highly related to LMX/TLS (L=0.48), LJU/TLS (L=0.16), LQJ/TLS (L=0.21), LQU/TLS (L=0.28), LSQ/TLS (L=0.20), SMX/TWS (L=0.33), WMX/TWS (L=0.30), WJU/TWS (L=0.26) and WQJ/TWS (L=0.41), which represent the highest values, as well as bones constituting both lateral and posterior emargination. Conversely, PC2 was mostly represented by LPA/TLS (L=0.67), LSQ/TLS (L=0.34) and WPA/TWS (L=0.33) (see Table 4). These loadings represent shape changes in regions of the skull that are associated with muscles' attachments as well as trituration surfaces (see below).

4. Discussion

4.1. The single population hypothesis

In this section, we discuss the single population hypothesis considering two fronts, one underlied on the taphonomy of the Tartaruguito locality, and another on the possibility of the skull variation represent one or more specimens of species *Roxochelys wanderleyi* in the sample, a shell-only species also found at the site.

4.1.1. The depositional context at the "Tartaruguito" site

347 The depositional environment at the Pirapozinho site is well-known from previous studies, which
348 point out to seasonal floods in which turtles might have gathered in water bodies for foraging,
349 followed by droughts that caused their death (Soares et al., 1980; Fulfaro and Perinotto, 1996;
350 Fernandes & Coimbra, 2000; Henriques et al., 2002, 2005; Suárez, 2002; Bertini et al., 2006;
351 Henriques, 2006). This is, consequently, a case of several seasonal non-selective death events,
352 with individuals representing semaphoronts connected temporally (between generations), thus
353 comprising a single population (agreeing with Futuyma, 1993 population definition and used by
354 Romano & Azevedo, 2007). We failed to disprove the null hypothesis that all individuals belong
355 to a same population of *Bauruemys elegans*, agreeing with Romano & Azevedo (2007)
356 conclusion using post-cranium data.

357 *4.1.2. Taxonomic considerations on the sample*

358 Many skulls sampled show taphonomic effects, such as cracks and crushing (Fig. 8). For
359 instance, MN7071-V is notably the largest specimen of the sample and is represented in the
360 uppermost positive side of the size-related PC2 axis (Fig. 6C). Although it is indeed a big
361 specimen, it was clearly a taphonomic effect (crushing) that caused it to be larger than it really
362 was (Fig. 8A). On the other hand, Bertini et al. (2006) indicated that turtle bodies have suffered
363 little transportation or crushing in Tartaruguito site. We agree with this taphonomical
364 interpretation of the site, as most specimens do not show huge breaks (Fig. 8B and 8C) that could
365 cause misinterpretation of the morphometric results (the case of MN7071-V is an exception in
366 our sample in this respect).

367 Another aspect is the presence of polymorphism in *B. elegans*. Romano (2008) presented an
368 unusual carapace for the specimen MN7017-V, as having a seventh neural bone, differing from

the diagnostic number of six neurals for this species, and with the diagnostic four-squared second neural bone not contacting first costals (Suarez, 1969; Kischlat, 1994; Gaffney et al., 2011). The morphometric analysis performed by Romano (2008) did not reveal significant statistical differences between MN 7017-V and other *B. elegans* specimens. We have included the MN7017-V skull in our analysis, and there was no variation to state anything apart from Romano's (2008) conclusion that it is probably a polymorphic *B. elegans* specimen (Fig. 6C). Still, we reevaluated this skull and found the diagnosticcharacters for *B. elegans*. Therefore, all skulls included in our study belong to the same species (i.e. *B. elegans*).

Among the five valid fossil turtle species found throughout the Bauru Basin, only two have been collected at the Pirapozinho site so far (Romano et al., 2013). The first is *B. elegans*, which is recognized by both skull and shell materials; the second is *Roxochelys wanderleyi* Price, 1953, based only on shell material (de Broin, 1991; Oliveira & Romano, 2007; Romano & Azevedo, 2007; Gaffney et al., 2011; Romano et al., 2013). So far, none *R. wanderleyi* with skull-shell associated body parts were collected, and thus we cannot claim that the skulls found at Tartaruguito site belong to this species until a skull-shell *R. wanderleyi* specimen be found, since all analyzed skulls can be safely identified as belonging to *B. elegans*.

4.2. Ontogenetic changes in *B. elegans* skull

Once we have assessed that all specimens belong to the same species and are likely from the same population, we are able to discuss the skull variation in the sample assuming as due to inter-populational variety. For the sake of organization, we divided the discussion into two parts, based on the anatomical regions of the turtle skull: upper temporal fossa and lower temporal fossa, following Schumacher (1973), Gaffney (1979) and Gaffney et al. (2006). We have chosen

this organization because the bones we found most associated with the principal components in the two PCA analyses constitute these two regions and are generally involved in aspects of the feeding mechanisms of turtles, either as muscles attachments or forming triturating surfaces.

4.2.1. Bones of the upper temporal fossa and skull roofing

The temporal emargination of podocnemidid turtles is formed by the dorsal, horizontal plate of the parietal, the quadratojugal and the squamosal, with no contribution of the postorbital (Gaffney, 1979; Gaffney et al., 2011). This region (and bones) is associated with the origin of the adductor muscle fibers (m. adductor complex; Fig. 9A and 9B) (Schumacher, 1973; Werneburg, 2011; Werneburg, 2012; Jones et al., 2012; Werneburg, 2013), which run through *cartilago transiliens* of the *processus trochlearis pterygoidei* of the pterygoid and insert at the coronoid process of the lower jaw (Schumacher, 1973; Gaffney, 1975; Gaffney, 1979; Lemell et al., 2000; Werneburg, 2011). These muscles promote the closure of the mouth, thus it is reasonable to associate the attachment surface to bite force and the latter to the prey hardness. Yet, on the ventral flange of the squamosal originates the m. depressor mandibulae (Schumacher, 1973; Gaffney et al., 2006; Werneburg, 2011; Fig. 9B), which causes the abduction (=opening) of the mandible.

The variation in this area of the skull in turtles was a matter of some studies (e.g. Dalrymple, 1977; Claude et al., 2004; Pfaller et al., 2011), which indicated allometric ontogenetic growth patterns of the bones in these regions. These authors were able to identify a high correlation with the increasing of muscle mass and shift in feeding features (Dalrymple, 1977; Pfaller et al., 2010; Pfaller et al., 2011). Moreover, there are changes in skull shape associated to the aquatic environment and foraging strategies, as suggested for emydid and testudinoid turtles by Claude

et al. (2004). Although these studies focused on hide-necked turtles, the same morphoecological patterns can be applied to side-necked turtles, since there are habitat occupation similarities between side-necked and hide-necked turtles with implications to the skull morphology due to morphofunctional constraints (Schumacher, 1973; Lemell et al., 2000), besides the adaptive selection regarding fresh water feeding strategies (see Lauder & Prendergast, 1992, Aerts et al., 2001 and Van Damme & Aerts, 2001 for feeding strategies in freshwater turtles).

The high variance and positive allometric growth of the parietal (LPA: a=0.38; WPA: a=0.32), quadratojugal (LQJ: a=0.16; WQJ: a= -0.06) and squamosal (LSQ: a=0.30) lead to an increase in temporal emargination and, consequently, a greater area for attachment of the m. adductor mandibulae externus. The consequence of this would be the generation of large forces and high velocities during the fast closing phase of an aquatic feeder, as seen in *Pelusios castaneus* (Lemell et al., 2000), and even a more powerful bite for crushing harder prey, as seen in *Sternotherus minor* (Pfaller et al., 2011). In addition, the lenghten of the squamosal would allow a greater insertion area of the m. depressor mandibulae and muscles of the hyobranchial apparatus (e.g. *m. constrictor colli*) (Schumacher, 1973; Gaffney, 1979; Claude et al., 2004; Gaffney et al., 2011; Werneburg, 2011). The *m. depressor mandibulae* is useful for an increased gape opening speed and the hyobranchial apparatus musculature is involved in backwards water flow generation by the lowering of the hyoid apparatus, two characteristics well reported for other pleurodire turtles as *Chelodina longicollis, Chelus fimbriatus* and *Pelusios castaneus* (e.g.Van Damme & Aerts, 1997; Aerts et al., 2001; Lemell et al., 2000; Lemell et al., 2002). Moreover, Claude et al. (2004) demonstrated that aquatic turtles with suction feeding mode possess longer skulls than terrestrial turtles, the squamosal being most prominent bone involved

435 in this elongation and functionally related to the style of prey capture (= suction) as a support for
436 mandible and hyoid muscles.

437 Also, Gaffney et al. (2011), in a comparison with other podocnemidid turtles, indicated *B.*
438 *elegans* as having a "skull relatively wide and flat" (p. 12), which could be observed by the
439 increasing of some bones, specially the postorbital (Figs. 3G and 4H), parietal (Fig. 3A and 3J),
440 quadratojugal (Figs.3I and 4F) and jugal (Figs. 3C and 5B). Comparing the postorbital allometry
441 (better discussed below) with those of the bones in contact with it in the skull roof (frontal,
442 parietal, jugal and quadratojugal; Gaffney et al., 2011), we observe an influence of the positive
443 growth of the former into the others, leading to flattening and widening of the skull.

444 In a study assessing the bite performance in turtles, Herrel et al. (2002) suggested that a higher
445 skull is efficient in promoting stronger bite forces, specially in species which feed on hard prey,
446 but they also pointed out that additions in bite forces may be achieved by "getting longer and
447 larger" skull with no increasing in skull height. Thus, in addition to provide gains in muscle
448 attachment area, by the growing of parietal, quadratojugal and squamosal, leading to a longer
449 skull, a stronger bite and possibly a change in diet along the ontogeny. Also, the allometric
450 growths of most of skull bones, particularly the positive allometry of the postorbital, suggests a
451 more roofed skull in *B. elegans* bigger adults. Given the allometric patterns aforementioned, *B.*
452 *elegans* may have had a wide and flat but long skull, which would have compensated the loss of
453 muscle volume and attachment area caused by widening and flattening the skull (Herrel et al.,
454 2002). Correlations between a more emarginated skull and increases in the volume of the
455 adductor muscles were also explored in a cranial evolutionary framework of stem-turtles by
456 Sterli and de la Fuente (2010).

457 At last, Gaffney et al. (2006, 2011) scored a character based upon the contact between
458 quadratojugal and parietal bones (char. 13 of Gaffney et al., 2006; char. 5 of Gaffney et al.,
459 2011). They also state that this contact is present in *Hamadachelys* + Podocnemididae clade,
460 with a large quadratojugal (state 1), in contrast to most of other Pelomedusoides (state 0: contact
461 absent, as seen in Pelomedusidae, Araripemydidae and many bothremydids (e.g.
462 Kurmademydini, Cearachelyini and Bothremydini); state 2: contact present with small
463 quadratojugal in some Taphrosphyini, Bothremydidae). Indeed *B. elegans* possess a large
464 quadratojugal, which means that the reduction of the postorbital evolved after *Bauruemys* node
465 of divergence, as confirmed in performed cladistic analyses. However, we found a greater
466 increasing (positive allometry) of the two measurements of the postorbital and this might have
467 influenced the growth of parietal and quadratojugal, as well as the jugal (see below), so that the
468 state 1 seen in *B. elegans* is possibly a consequence of allometric changes. This is easily seen
469 when comparing the enatiometry of the width of the quadratojugal (WQJ: a=-0.06) and the slight
470 increasing in the length of this bone (LQJ: a=0.16) with the postorbital measurements. It also
471 could have influenced the growth of the parietal, but to a lesser extent, as seen in the allometries
472 of this bone (LPA: a=0.38; WPA: a=0.32).

473 When comparing the stem-Podocnemidinura species (i.e. *Brasilemys*, *Hamadachelys*) and stem-
474 Podocnemididae (e.g. *Bauruemys*, *Peiropemys*, *Pricemys* and *Lapparentemys*), with the
475 Podocnemidodda (i.e. Podocnemidand + Erymnochelydand) (Gaffney et al., 2011; Fig. 8), it is
476 clear that an increasing in the parietal-quadratojugal contact has occurred along the
477 podocnemidid lineage, and consequently led to a more roofed and less emarginated skull. We
478 suggest that in *B. elegans* the small contact is due to the positive growth of the postorbital
479 resulting in a more emarginated skull than other podocnemidids, as described by Gaffney et al.

(2011). Yet, within Podocnemidoddathis bone suffered the opposite effect (i.e. small growth), showing variations in size and even being absent in some species (e.g. *Podocnemis sextuberculata*; Ruckes, 1937; Gaffney, 1979; Gaffney et al., 2011), though the emargination is still great. On the other hand, in Erymnochelydand the postorbitals are large but the quadratojugal and parietal are large as well, leading to a greater contact between these bones and a well-roofed but less emarginated skull, being a reversion in *Bairdemys venezuelensis* and *B. sanchezi* within Erymnochelydand (Gaffney et al., 2011). Therefore, the increase or decrease in the temporal emargination within Podocnemididae could be due to variation of allometric patterns in bones that form the skull roof, particularly the postorbital, quadratojugal, and parietal, among different lineages. Given that observation, we speculate that characters related to the form of the aforementioned bones (postorbital, squamosal, and parietal) are potencially more susceptible to homoplasy.

4.2.2. Bones of the lower temporal fossa

The lower adductor chamber in Pelomedusoides is formed externally and laterally by the jugal and quadratojugal, with the addition of the maxilla in some cases (e.g.: *Podocnemis* spp. and *Bairdemys sanchezi*). The well developed cheek emargination, found in most but not all podocnemidid turtles (the exceptions are allErymnochelydand, but *Bairdemys* spp., *Cordichelys antiqua* and *Latentemys plowdeni*), is also part of the adductor chamber (Gaffney, 1979; Gaffney et al., 2006; Gaffney et al., 2011). Internally and medially, the postorbital, the jugal, and the pterygoid compose the *septum orbitotemporale*, partially separating the *fossa orbitalis* from the *fossa temporalis*; along with the palatine, they aid to support the *processus trochlearis pterygoidei* of the pterygoid (Gaffney, 1975; Gaffney 1979; Gaffney et al., 2006). There is a passage medially to the process of the pterygoid and the *septum orbitotemporale*, running from

503 the *fossa orbitalis* to the *fossa temporalis*, the *sulcus palatinopterygoideus*. The palatine and
504 pterygoid form the floor of its passage, whereas the parietal, postorbital and frontal limit its
505 upper portion. In this region, the *m. adductor mandibulae* fibers run through the *processus*
506 *trochlaris pterygoidei*, and the *m. adductor mandibulae internus* (i.e. *m. pterygoideus* and *pars*
507 *pseudotemporalis*; Fig. 9B) mostly originates throughout the pterygoid and parietal bones
508 (Schumacher, 1973; Lemell et al., 2000; Lemell et al., 2002; Werneburg, 2011). The *m. adductor*
509 *mandibulae internus* fibers are involved in the jaw-closure system by generating counter forces
510 (protraction) to the *m. adductor mandibulae externus* (retraction) (Schumacher, 1973; Lemell et
511 al., 2000; Lemell et al., 2002; Fig. 9C and 9D).

512 Variation of the upper temporal fossa has been studied in different turtles, such as various
513 trionychids (Dalrymple, 1977) and *Chelydra serpentina* (Herrel et al., 2002). However, few
514 studies report the variation of the lower adductor chamber, although both the upper and lower
515 temporal fossa are anatomically and functionally coupled (Schumacher, 1973). Dalrymple (1977)
516 identified a positive allometry in the width of the "temporal passageway" in trionychids. This
517 area is related to the cryptodire pulley system (i.e. a *processus trochlearis* formed by the
518 quadrate and opisthotic) and is analogous to the pleurodire pterygoid process, and thus can be
519 comparable functionally (Gaffney, 1979). Herrel et al. (2002) concluded that the increase of the
520 bite force in turtles is due to either the increased height of the skull, leading to a more open angle
521 of the *processus trochlearis* in relation to skull longitudinal axis, or to enlargement (in width and
522 length) of the skull, because it allows more area for muscle attachment and volume. We observed
523 the same pattern of growth change in *B. elegans*, as evidenced by the positive allometry of the
524 parietal, postorbital, palatine and pterygoid bones. Other features were observed by Dalrymple
525 (1977) in trionychids (e.g. height and width of the supraoccipital crest, lengthening of the

526 squamosal crest and a development of a horizontal crest in the parietal) and were correlated to
527 changes in skull shape with a shift in feeding habits, from softer to harder preys as individuals
528 age. Again, this seems to be the case in *B. elegans*, as evidenced by the positive allometry of the
529 squamosal and parietal bones.

530 The bones that mainly compose the skull rostrolaterally and the lateral emargination revealed a
531 correlated allometric shape shift. Even so, jugal and maxilla showed small allometric variation
532 (Figs. 4B, 4C, 6A, and 6B). The reduction of the jugal (WJU: a= -0.23) and quadratojugal (WQJ:
533 a= -0.06) along with the small growth of the maxilla (WMX: a=0.19) demonstrate a decrease in
534 height at the anterior portion of the skull. Because of the contact between jugal and quadratojugal
535 with the postorbital (and its increase; see previous topic), we suggest that the latter would
536 possibly has affected the growth of the former bones. Moreover, the strong development of the
537 postorbital would ultimately affect the width of the maxilla, which in turn would also affect the
538 jugal. In contrast, the lengthen of this bone would be less affected (LMX: a=0.39). In addition,
539 there is a considerable increment in the stretch of maxilla (SMX: a=0.70) (Fig. 3H) leading to a
540 broader rostrum. Yet, this could allow a greater area for crushing, as observed by Kischlat (1994)
541 for *B. elegans*, but also related to ontogenetic growth (pers. obs.). All these allometric changes
542 indicate that *B. elegans* owns a more flattened and wider skull (Gaffney et al., 2011), which
543 could have allowed greater bite forces generation (Herrel et al., 2002).

544 There are other morphological implications in which the lower adductor chamber bones are
545 involved and that are worth discussing. As previously pointed out, three bones compose the
546 *septum orbitotemporale*: pterygoid, jugal, and postorbital (Gaffney, 1979; Gaffney et al., 2006).
547 Together with the palatine, these three bones provide support for the *processus trochlearis*
548 *pterygoidei*, whereupon runs the tendon that connect the m. adductor externus complex into the

549 lower jaw (Schumacher, 1973; Gaffney, 1975; Gaffney 1979; Lemell et al., 2000; Gaffney et al.,
550 2006; Werneburg, 2011). Nearby the process, many muscle fibers originate or cross towards
551 their insertions points (Schumacher, 1973; Werneburg, 2011). The temporal emargination at the
552 upper adductor chamber becomes more emarginted during growth. As a consequence, the
553 attachment area for *m. adductor mandibulae externus* increase during aging, potentially
554 generating stronger bite forces. The consequence of this temporal emargination indentation is
555 that the trochlear process would must become more robust to support higher forces. We interpret
556 that the positive allometries of pterygoid (LPT a=1.37), postorbital (LPO a=1.25 and WPO
557 a=1.36), and palatine (LPAL a=1.11) could be a response to this robustness of the trochlerar
558 process during growth. In other words, they would act together by giving more resistance to the
559 area in which the high forces created by the *m. adductor mandibulae externus* are applied.
560 Gaffney (1979) suggested this robustness occurs because muscle volume increase and,
561 consequently, higher bite forces, so these three bones would reinforce the *septum*
562 *orbitotemporale* in order to support and do not break when muscles are contracted. In addition to
563 such reinforcement, the growth of palatine could be associated with a larger area for crushing
564 preys such as mollusks and crustaceans, as pointed out by Kischlat (1994).

565 The *m. adductor mandibulae internus* and *m. adductor mandibulae posterior* (Fig. 9B), which
566 originate at the quadrate, prootic, pterygoid, palatine, postorbital and the descending process of
567 the parietal (Schumacher, 1973; Werneburg, 2011), are important during the jaw-closure phase.
568 The importance of these muscles has been debated for early tetrapods with flat skull and aquatic
569 lifestyle (e.g. Temnospondyli and Lepospondyli; Frazzetta, 1968), in which the internal muscle
570 might have assumed the main function of closing the jaw (Werneburg, 2012). This also occurs in
571 turtles with flat skulls and with poorly developed *crista supraoccipitalis* (e.g. Chelidae;

572 Werneburg, 2011; Werneburg, 2012). However, *B. elegans* does not have a skull as flat as
573 chelids, but has a long supraoccipital bone as well as a greater temporal emargination (Gaffney et
574 al., 2011), indicating more area and volume availableto *m. adductor mandibulae externus*
575 (Dalrymple, 1977; Sterli & de la Fuente, 2010). The mechanical effects of adductor muscles
576 upon the lower jaw during food capture has been demonstrated in some turtles (Schumacher,
577 1973; Lemell et al., 2000; Lemell et al., 2002; Pfaller et al., 2011). These studies agree that
578 besides acting to close the mouth, the *m. adductor mandibulae internus* executes counter
579 protraction forces to the *m. adductor mandibulae externus* retraction forces, while *m. adductors*
580 *mandibulae posterior* produce medial forces (Fig. 10C and 10D). The contraction of all these
581 muscles together avoid displacements of the mandible and reduce stresses at the articulation
582 (Schumacher, 1973; Lemell et al., 2000; Lemell et al., 2002). The positive allometries of the
583 bones of the lower adductor chamber of *B. elegans*, therefore, may reflect greater resistance for a
584 more robust musculature of *m. adductor mandibulae internus* and *m. adductor mandibulae*
585 *posterior* in response to higher forces created by external adductors. Besides, these muscles also
586 play the main role in feeding, as proposed for aquatic feeders (Frazzetta, 1968; Werneburg,
587 2012), in addition to a larger area between the two tips of the maxilla (i.e. SMX a=0.70) and a
588 flattened skull.

589 **4.3. Feeding changes over ontogeny in *B. elegans***

590 Changes in skull shape may be due to habitat differences in which terrestrial turtles (e.g.
591 testudinids) possess higher and shorter skulls while aquatic turtles (e.g. emydids) have flatter and
592 longer skulls (Claude et al., 2004). The changes in skull shape of turtles along ontogeny have
593 been assessed in living species (Dalrymple, 1977; Pfaller et al., 2011). Generally, it is supported
594 that a diet shift occurs from small soft prey to bigger harder ones, in association with higher,

595 larger and more robust skulls. These, in turn, are more suitable for crushing clams and/or to
596 capture fishes by having a greater gape. The overall aquatic morphology comprises adaptations
597 to suction feeding, which was also discussed by Herrel et al. (2002), and could be the case of *B.*
598 *elegans*. Firstly because taphonomic studies at Pirapozinho site suggested a riverine ephemerous
599 system (Soares et al., 1980; Fulfaro and Perinotto, 1996; Fernandes & Coimbra, 2000; Henriques
600 et al., 2002, 2005; Suárez, 2002; Bertini et al., 2006; Henriques, 2006) and fossils that suffered
601 little transportation (Bertini et al., 2006), thus it is more likely that *B. elegans* has been a semi-
602 aquatic turtle, similar to the extant freshwater turtles. Secondly, the general pattern observed
603 revealed form and shape changes in both temporal and lateral emargination (upper and lower
604 adductor chamber, respectively): as a whole, *B. elegans* skull seems to become more
605 emarginated, flattened and longer as it grows, according to the skull shape for aquatic turtles
606 found by Claude et al. (2004), and indicating greater area and volume for muscles attachment. In
607 addition, the deeper temporal emargination of *B. elegans* indicates a greater increase in muscle
608 volume (Kischlat, 1994), thus leading to a stronger bite force (Sterli & de la Fuente, 2010). This
609 leads us to interpret such changes as related to a shift in diet as individuals grow instead of a shift
610 in habitat.

611 Malvasio et al. (2003) described diet changes in *Podocnemis expansa*, *P. unifilis* and *P.*
612 *sexturberculata* due to aging, concluding that the latter is a carnivore species, whereas the two
613 former are omnivorous. Whereas *P. expansa* changes its diet becoming more herbivorous, *P.*
614 *unifilis* remains more balanced with similar ingestion of vegetables and meat (Malvasio et al.,
615 2003). Kischlat (1994) suggested that *B. elegans* might have fed of hard preys and, given the
616 several mollusk and crustacean species described for the Pirapozinho site (Dias-Brito et al.,
617 2001), it might have composed the diet of *B. elegans*. In this context, we agree with Kischlat

(1994) and suggest that smaller juveniles individuals might have fed on less hard and small food items (e.g. snails and small fishes) whereas bigger old specimens fed on harder and larger preys, such as crustaceans and bigger mollusks.

Although there is a possibility that size differences could be due to sexual dimorphism (R. Hirayama and S. Thomson, pers. comm.) as aforementioned (see Introduction, section 1.2.3), we were not able to assume such assumption. Furthermore, if there is size-related dimorphism, it would imply on potential diet differentiation between adults male and female of *B. elegans*. Since we were not able to determine size-related sexual dimorphism, such statementis merely speculative.

5. Conclusions

As Romano & Azevedo (2007) (for shell material), our data did not show enough morphometrical variation to suggest population differences among our sample. So, we did not have evidence to disprove that the "Tartaruguito" site is composed of a single population of *B. elegans*. However, it is feasible to assume that different generations of individuals were crowded in this locality by the accumulation of corpses due to several drying events as previously suggested by Henriques et al. (2005) and Henriques (2006). Since none *B. elegans* hatchling were found in the “Tartaruguito” site until now, it might have been preferentially a freshwater foraging area.

As regards to the morphometric data, the observed variation and allometries in the skull bones, mainly the PA, QJ, SQ, QU, PO, JU, MX, PAL and PT, as well as PCAs loadings, reflect shape differences in both upper and lower adductor chambers. We interpret this allometric variation as

an indicative of more area attachment and resistance for stronger adductor muscles, which are accompanied by changes in diet during aging, from softer to harder prey, as seen in living turtlesspecies.

As regards to the use of images for carrying out morphometrics studies, we conclude that the use of calipers can be replaced by softwares that work on images. ImageJ is a useful and time-saving tool for this matter. However, one needs to beware when measuring straight lines between landmarks that are located in different depths, which result in angled lines against the projection orthogonal plane. Unattention to this detail will lead to assess lower values for a given measurement than its real size.

Regarding the approaches applied to our data to deal with missing entries in the matrix (i.e. mean value or iterative imputation), both were useful for answering the questions we raised (i.e. the single population hypothesis), though little different results were obtained (few specimens out of 95% confidence ellipse in mean value approach in contrast with none specimen out of ellipse in iterative imputation approach). However, we recommend the iterative imputation as the most appropriate approach to deal with missing data in paleontological studies on the basis of the statistical assumptions it was developed (a sample-based regression for characters estimation) and the more conservative results.

Institutional Abbreviations: AMNH – American Museum of Natural History, New York, NY, United States; **LPRP –** Laboratório de Paleontologia da Faculdade de Filosofia, Ciências e Letras de Ribeirão Preto, Universidade de São Paulo, Ribeirão Preto, SP, Brazil; **MN –** Museu Nacional, Universidade Federal do Rio de Janeiro, Rio de Janeiro, RJ, Brazil; **MCT –** Museu de Ciências da Terra, Departamento Nacional de Produção Mineral, Rio de Janeiro, RJ, Brazil;

662 **MCZ –** Museum of Comparative Zoology, Harvard University, Cambridge, MA, United States;
663 **MZSP -** Museu de Zoologia, Universidade de São Paulo, São Paulo, SP, Brazil.

664 **Anatomical abbreviations: PF –** prefrontal; **FR –** frontal; **PA –** parietal; **VO –** vomer; **PAL –**
665 palatine; **PT –** pterygoid; **BS –** basisphenoid; **BO –** basioccipital; **MX –** maxilla; **JU –** jugal; **QJ**
666 **–** quadratojugal; **QU –** quadrate; **PO –** postorbital; **SQ –** squamosal; **OP –** opisthotic; **CO –**
667 choanal.

668 **Measurements abbreviations: TLS –** Total length of skull; **LPF –** Length of prefrontal; **LFR –**
669 Length of frontal; **LPA –** Length of parietal; **LVO –** Length of vomer; **LPAL –** Length of
670 palatine; **LPT –** Length of pterygoid; **LBS –** Length of basisphenoid; **LBO –** Length of
671 basioccipital; **LMX –** Length of maxilla; **LJU –** Length of jugal; **LQJ –** Length of
672 quadratojugal; **LQU –** Length of quadrate; **LPO –** Length of postorbital; **LSQ –** Length of
673 squamosal; **TWS –** Total width of skull; **WPF –** Width of prefrontal; **WFR –** Width of frontal;
674 **WPA –** Width of parietal; **SMX –** Stretch of maxilla; **WVO –** Width of vomer; **WCO –** Width
675 of choanal; **WPAL –** Width of palatine; **WBS –** Width of basisphenoid; **WMX –** Width of
676 maxilla; **WJU –** Width of jugal; **WQJ –** Width of quadratojugal; **WPO –** Width of postorbital;
677 **WOP –** Width of opisthotic.

678 **Acknowledgments**

679 We are grateful to Sergio Azevedo, Deise Henriques, Luciana Carvalho, Lílian Cruz (DGP/MN)
680 and Max Langer (LPRP/USP) for allowingthe loan of the material and/or visits to collections
681 under their care when necessary. Pedro Romano thanks the following people and institutions for
682 facilitating access to collections: E. Gaffney, C. Mehling and F. Ippolito (AMNH); and R.
683 Cassab and R. Machado (MCT). We thank to Gustavo Oliveira (UFRPE) for being part of

Thiago Mariani's undergraduate thesis committee and for making revisions, suggestions, and comments that contributed to this paper. We are also grateful to M. Lambertz (University of Bonn) and C. Mariani for revisions and comments on early versions of the manuscript. Gabriel Ferreira (LPRP/USP), Mirian Menegazzo (Unesp) and Gustavo Oliveira (UFRPE) shared information about Bauru Basin fossil turtle records that were incorporated to figure 1. Torsten Scheyer and a second anonymous reviewer provided comments and insights that greatly improved the manuscript. Preliminary results of this paper composed the undergraduate thesis of Thiago Mariani.

6. References

AERTS P, VAN DAMME J, HERREL A. 2001. Intrinsic mechanics and control of fast cranio-cervical movements in aquatic feeding turtles. American Zoologist 41:1299-1310. DOI: dx.doi.org/10.1668/0003-1569(2001)041[1299:IMACOF]2.0.CO;2.

AGUILERA OA. 2004. Tesoros Paleontológicos de Venezuela. Urumaco, Patrimonio Natural de la Humanidad. Editorial Arte: Caracas.

ANQUETIN J. 2012. Reassessment of the phylogenetic interrelationships of basal turtles (Testudinata). Journal of Systematic Paleontology 10(1):3-45. DOI: 10.1080/14772019.2011.558928.

BAILEY SE. 2004. A morphometric analysis of maxillary molar crowns of Middle-Late Pleistocene hominins. Journal of Human Evolution 47(3): 183-198. DOI: dx.doi.org/10.1016/j.jhevol.2004.07.001.

BERTINI RJ, SANTUCCI RM, TOLEDO CEV, MENEGAZZO MC. 2006. Taphonomy and depositional history of an Upper Cretaceous turtle-bearing outcrop from the Adamantina Formation, Southwestern São Paulo state. Revista Brasileira de Paleontologia 9(2):181-186.

CADENA EA, BLOCH JI, JARAMILLO CA. 2010. New podocnemidid turtle (Testudines: Pleurodira) from the Middle-Upper Paleocene of South America. Journal of Vertebrate Paleontology 30(2):367-382. DOI: dx.doi.org/10.1080/02724631003621946.

CADENA EA, BLOCH JI, JARAMILLO CA. 2012. New bothremydid turtle (Testudines, Pleurodira) from the Paleocene of Northeastern Colombia. Journal of Paleontology 86(4):688-698. DOI: dx.doi.org/10.1666/11-128R1.1.

713 CADENA EA, KSEPKA DT, JARAMILLO CA, BLOCH JI. 2012. New pelomedusoid turtles
714 from the late Paleocene Cerrejón Formation of Colombia and their implications for phylogeny
715 and body size evolution. Journal of Systematic Paleontology 10(2):313-331. DOI:
716 dx.doi.org/10.1080/14772019.2011.569031.

717 CAMPOS DA, OLIVEIRA GR, FIGUEIREDO RG, RIFF D, AZEVEDO SAK, CARVALHO
718 LB, KELLNER AWA. 2011. On a new peirosaurid crocodyliform from the Upper Cretaceous,
719 Bauru Group, southeastern Brazil. Anais da Academia Brasileira de Ciências 83(1):317-327.
720 DOI: dx.doi.org/10.1590/S0001-37652011000100020.

721 CLAUDE J, PRITCHARD PCH, TONG H, PARADIS E, AUFFRAY JC. 2004. Ecological
722 correlates and evolutionary divergence in the skull of turtles: a geometric mophometric
723 assessment. Systematic Biology 53(6):933-962. DOI: 10.1080/10635150490889498.

724 CONGDON JD, NAGLE RD, KINNEY OM, SELS RCVL, QUINTER T, TINKLE DW. 2003.
725 Testing hypotheses of aging in long-lived painted turtles (Chrysemys picta). Experimental
726 Gerontology 38:765-772.

727 DALRYMPLE GH. 1977. Intraspecific variation in the cranial feeding mechanism of turtles of
728 the genus *Trionyx* (Reptilia, Testudines, Trionychidae). Journal of Herpetology 11(3):255-285.
729 DOI: 10.2307/1563241.

730 DEPECKER M, RENOUS S, PENIN X, BERGE C. 2005. Procrustes analysis: a tool to
731 understand shape changes of the humerus in turtles (Chelonii). Comptes Rendus Palevol 5: 509-
732 518.

733 DEPECKER M, BERGE C, PENIN X, RENOUS S. 2006. Geometric morphometrics of the
734 shoulder girdle in extant turtles (Chelonii). Journal of Anatomy 208: 35-45.

735 DE BROIN F. 1991. Fossil turtles from Bolivia. In: Suarez-Soruco R. *Fossiles y facies de*
736 *Bolívia – Vol. I Vertebrados*. Revista Técnica de YPFB, 12(3-4): 509-527.

737 DE LA FUENTE MS, STERLI J, MANIEL I. 2014. Origin, evolution and biogeographic history
738 of South American turtles. Springer Earth System Sciences.

739 FERNANDES LB, COIMBRA AM. 2000. Revisão estratigráfica da parte oriental da Bacia
740 Bauru (Neocretáceo). Revista Brasileira de Geociências 30(4):717-728.

741 FERREIRA GS, RINCÓN AD, SOLÓRZANO A, LANGER MC. 2015. The last marine
742 pelomedusoids (Testudines: Pleurodira): a new species of *Bairdemys* and the paleoecology of
743 Stereogyina. PeerJ 3:e1063. DOI: 10.7717/peerj.1063.

744 FRANÇA MAG, LANGER MC. 2005. A new freshwater turtle (Reptilia, Pleurodira,
745 Podocnemidae) from the Upper Cretaceous (Maastrichtian) of Minas Gerais, Brazil.
746 Geodiversitas 27: 391-411.

747 FRAZZETTA TH. 1968. Adaptative problems and possibilities in the temporal fenestration of
748 tetrapod skulls. Journal of Morphology 125:145-157.

749 FULFARO VJ, PERINOTTO JAJ. 1996. A Bacia Bauru: estado da arte. Boletim do Quarto
750 Simpósio sobre o Cretáceo do Brasil, UNESP, Rio Claro, SP: 297-303.

751 FUTUYMA DJ. 1993. *Biologia evolutiva*. 2 ed. Ribeirão Preto: FUNPEC-RP.

752 GAFFNEY ES. 1972. An Illustred Glossary of Turtle Skull Nomeclature. American Museum
753 Novitates 2486:33pp.

754 GAFFNEY ES. 1975. A phylogeny and classification of the higher categories of turtles. Bulletin
755 of the Americam Museum of Natural History 155(5):387-436.

756 GAFFNEY ES. 1979. Comparative Cranial Morphology of Recent and Fossil Turtles. Bulletin of
757 the American Museum of Natural History 164(2):65-376.

758 GAFFNEY ES, MEYLAN PA, WOOD RC, SIMONS E, CAMPOS DA. 2011. Evolution of the
759 side-necked turtles: the family Podcnemididae. Bulletin of the American Museum of Natural
760 History 350: 237pp. DOI: dx.doi.org/10.1206/350.1.

761 GAFFNEY ES., MEYLAN PA, WYSS AR. 1991. A computer assisted analysis of the
762 relationships of the higher categories of turtles. Cladistics 7:313-335. DOI: 10.1111/j.1096-
763 0031.1991.tb00041.x.

764 GAFFNEY ES, SCHEYER TM, JOHNSON KG, BOCQUENTIN J, AGUILERA OA. 2008.
765 Two new species of the side necked turtle genus, *Bairdemys* (Pleurodira, Podocnemididae), from
766 the Miocene of Venezuela. Palaontoloqische Zeitschrift 82(2):209-229.

767 GAFFNEY ES, TONG H, MEYLAN PA. 2006. Evolution of the sidenecked turtles: the families
768 Bothremydidae, Euraxemydidae and Araripemydidae. Bulletin of the American Museum of
769 Natural History 300:698pp. DOI: dx.doi.org/10.1206/0003-
770 0090(2006)300[1:EOTSTT]2.0.CO;2.

771 GOULD SJ. 1966. Allometry and size in ontogeny and phylogeny. Biological Reviews 41:587-
772 640. DOI: 10.1111/j.1469-185X.1966.tb01624.x.

773 GOULD SJ. 1979. An allometric interpretation of species-area curver: the meaning of the
774 coefficient. The American Naturalist 114(3):335-343.

775 HAMMER Ø, HARPER DAT, RYAN PD. 2001. Past: Palentological Statistics software
776 package for education and data analysis. Palaeontologia Electronica 4(1):9pp.

777 HAMMER Ø, HARPER DAT. 2006. *Paleontological Data Analysis*. Blackwell.

778 HENNIG, W. 1966. *Phylogenetic Systematics*. Urbana: University of Illinois Press.

779 HENRIQUES DDR. 2006. Sítio fossilífero de Pirapozinho: estudo de aspectos taxonômicos
780 através da análise básica e do exame de tomografia computadorizada. D. Phil. Thesis. Museu
781 Nacional – Universidade Federal do Rio de Janeiro.

782 HENRIQUES DDR, SUÁREZ JM, AZEVEDO SAK, CAPILLA R, CARVALHO LB. 2002. A
783 brief note on the paleofauna of "Tartaruguito" site, Adamantina Formation, Bauru Group, Brazil.
784 Anais da Academia Brasileira de Ciências 74(2): 366.

785 HENRIQUES DDR, AZEVEDO SAK, CAPILLA R. SUÁREZ JM. 2005. The Pirapozinho Site
786 – a taphofacies study. Journal of Vertebrate Paleontology 25:69A.

787 HERMANSON G, FERREIRA GS, LANGER MC. 2016. The largest Cretaceous
788 podocnemidoid turtle (Pleurodira) revealed by an isolated plate from the Bauru Basin, south-
789 central Brazil. Historical Biology 28(8):1-8. DOI: dx.doi.org/10.1080/08912963.2016.1248434

790 HERREL A, O'REILLY JC, RICHMOND AM. 2002. Evolution of bite performance in turtles.
791 Journal of Evolutionary Biology 15:1083-1094. DOI: 10.1046/j.1420-9101.2002.00459.x.

792 HUXLEY JS. 1950. Relative growth and form transformation. Proceedings of the Royal Society
793 of London B 137:465-469. DOI: 10.1098/rspb.1950.0055.

794 HUXLEY JS, TEISSIER G. 1936. Terminology of Relative Growth. Nature 137:780-781. DOI:
795 10.1038/137780b0.

796 ILIN A, RAIKO T. 2010. Practical approaches to Principal Components Analysis in the presence
797 of missing values. Journal of Machine Learning Research 11:1957-2000.

798 JARAMILLO CA, BAYONA G, PARDO-TRUJILLO A, RUEDA M, TORRES V,
799 HARRINGTON GJ, MORA G. 2007. The palynology of the Cerrejón formation (Upper
800 Paleocene) of northern Colombia. Palynology 31(1):153-189. DOI:
801 10.1080/01916122.2007.9989641.

802 JOLICOEUR P, MOSIMANN JE. 1960. Size and shape variation in the painted turtle: a
803 Principal Component Analysis. Growth 24: 339-354.

804 JONES MEH, WERNEBURG I, CURTIS N, PENROSE R, O'HIGGINS P, FAGAN MJ,
805 EVANS SE. 2012. The head and neck anatomy of sea turtles (Cryptodira: Chelonioidea) and
806 skull shape in Testudines. PloS ONE 7(11):e47852. DOI: 10.1371/journal.pone.0047852. DOI:
807 10.1371/journal.pone.0047852.

808 JOYCE WG. 2007. Phylogenetic relationships of Mesozoic turtles. Bulletin of Peabody Museum
809 of Natural History 48(1):3-102. DOI: dx.doi.org/10.3374/0079-
810 032X(2007)48[3:PROMT]2.0.CO;2.

JOYCE WG, LYSON TR. 2010. A neglected lineage of North American turtles fills a major gap in the fossil record. Paleontology 53(2): 241-248. DOI: 10.1111/j.1475-4983.2009.00929.x

KISCHLAT EE. 1994. Observações sobre *Podocnemis elegans* Suaréz (Chelonii, Pleurodira, Podocnemididae) do Neocretáceo do Brasil. Acta Geologica Leopoldensia, 39: 345-351.

KISCHLAT EE, BARBARENA, MC, TIMM, LL. 1994. Considerações sobre a queloniofauna do Grupo Bauru, Neocretáceo do Brasil [Boletim do Simpósio sobre o Cretáceo do Brasil, Rio Claro: Universidade Estadual Paulista. 105-107.

KISCHLAT EE. 2015. A new pleurodire turtle (Chelonii) from Adamantina Formation (Bauru Group), Upper Cretaceous of Brazil. PeerJ PrePrints 3:e1075. DOI: 10.7287/peerj.preprints.873v1.

KLINGER RC, MUSICK JA. 1995. Age and growth of loggerhead turtles (*Caretta caretta*) from Chesapeake Bay. Copeia 1:204-209.

KRZANOWSKI WJ. 1979. Between-Groups comparison of Principal Components. Journal of the American Statistical Association 74: 703-707.

KRZANOWSKI WJ. 1979. Between-Groups comparison of Principal Components – some sampling results. Journal of Statistical Computation Simulation 15: 141-154.

LEMELL P, BEISSER CJ, WEISGRAM J. 2000. Morphology and function of the feeding apparatus of *Pelusios castaneus* (Chelonia; Pleurodira). Journal of Morphology 244:127-135. DOI: 10.1002/(SICI)1097-4687(200005)244:2<127::AID-JMOR3>3.0.CO;2-U.

LEMELL P, LEMELL C, SNELDERWAARD P, GUMPENBERGER M, WOCHESLÄNDER R, WEISGRAM J. 2002. Feeding patterns in *Chelus fimbriatus* (Pleurodira: Chelidae). The Journal of Experimental Biology 205:1495-1506. PubMed: 11976360.

LYSON TR, JOYCE WG. 2009. A new species of *Palatobaena* (Testudines: Baenidae) and a maximum parsimony and bayesian phylogenetic analysis of Baenidae. Journal of Paleontology 83(3): 457-470. DOI: dx.doi.org/10.1666/08-172.1.

MARIANI TF, ROMANO PSR. 2014. Quando não podemos usar paquímetro: ImageJ como ferramenta para obtenção de dados morfométricos em fósseis [abstract no. 61]. Boletim de Resumos do IX Simpósio Brasileiro de Paleontologia de Vertebrados.

MALVASIO A, SOUZA AM., MOLINA FB, SAMPAIO FA. 2003. Comportamento e preferência alimentar em *Podocnemis expansa* (Schweigger), *P. unifilis* (Troschel) e *P. sextubeculata* (Cornalia) em cativeiro (Testudines, Pelomedusidae). Revista Brasileira de Zoologia, 20(1):161-168. DOI: dx.doi.org/10.1590/S0101-81752003000100021.

MENEGAZZO MC, BERTINI RJ, MAZINI FF. 2015. A new turtle from the Upper Cretaceous Bauru Group of Brazil, updated phylogeny and implications for age of the Santo Anastácio Formation. Journal of South American Earth Science 58: 18-32. DOI: 10.1016/j.jsames.2014.12.008.

MINGOTI SA. 2013. Análise de dados através de métodos de estatística multivariada: uma abordagem aplicada. Editora UFMG.

MURPHY EC, HOGANSON J, JOHNSON K. 2003. Lithostratigraphy of the Hell Creek Formation of North Dakota. In: Hartman JH, Johnson KR, and Nichols DJ ed, *The Hell Creek Formation and Cretaceous-Tertiary Boundary in the Great Plains: An Integrated Continental Record of the End of the Cretaceous*. The Geological Society of America, Special Paper 361. 9–34.

NORELL MA, WHEELER WC. 2003. Missing entry replacement data analysis: a replacement approach to dealing with missing data in paleontological and total evidence data sets. Journal of Vertebrate Paleontology 23(2): 275-283.

OLIVEIRA GR. 2011. Filogenia e descrição de novos Podocnemididae (Pleurodira: Pelomedusoides). D. Phil. Thesis. Museu Nacional – Universidade Federal do Rio de Janeiro.

OLIVEIRA GR, ROMANO PSR. 2007. Histórico dos achados de tartarugas fósseis do Brasil. Arquivos do Museu Nacional 65(1):113-133.

PARSONS TS, WILLIAMS EE. 1961. Two Jurassic turtle skulls: a morphological study. Bulletin of the Museum of Comparative Zoology 125(3):41-107.

PERES-NETO PR, JACKSON DA, SOMERS KM. 2003. Giving meaningful interpretation to ordination axes: assessing loading significance in Principal Component Analysis. Ecology 84(9): 2347-2363.

PFALLER JB, GIGNAC PM, ERICKSON GM. 2011. Ontogenetic changes in jaw-muscle architecture facilitate durophagy in turtle *Sternotherus minor*. Journal of Experimental Biology 214:1655-1667. DOI: 10.1242/jeb.048090.

PFALLER JB, HERRERA ND, GIGNAC PM, ERICKSON GM. 2010. Ontogenetic scaling of cranial morphology and bite-force generation in the loggerhead musk turtle. Journal of Zoology 280:280-289. DOI: 10.1111/j.1469-7998.2009.00660.x.

PRICE IL. 1953. Os quelônios da Formação Bauru, Cretáceo terrestre do Brasil meridional. Rio de Janeiro: Departamento Nacional de Produção Mineral/Divisão de Geologia e Mineralogia, 34pp. (Boletim 147).

RABI M, ZHOU CF, WINGS O, GE S, JOYCE WG. 2013. A new xinjiangchelyid turtle from the Middle Jurassic of Xinjiang, China and the evolution of the basipterygoid process in Mesozoic turtles. BMC Evolutionary Biology 13:203. DOI: 10.1186/1471-2148-13-203.

RASBAND WS. 1997. ImageJ, U.S.National Institutes of Health, Bethesda, Maryland, USA. *Avaiable at https://imagej.nih.gov/ij/*1997-2012.

RIEPPEL O. 1993. Patterns of Diversity in the Reptilian Skull. In: Hanken J, Hall BK, *The Skull, Vol. 2: Patterns of Structural and Systematic Diversity*. Chicago: The University of Chicago Press, 344-390.

RIFF D, ROMANO PSR, OLIVEIRA GR, AGUILERA OA. 2010. Neogene crocodile and turtle fauna in northern South America. In: Hoorn C, Wesselingh FP ed. *Amazonia, Landscape and Species Evolution: A Look into the Past*. Wiley-Blackwell Publishing. 259-280.

ROMANO PSR. 2008. An unusual specimen of *Bauruemys elegans* and its implication for the taxonomy of the side-necked turtles from Bauru Basin (Upper Cretaceous of Brazil). Journal of Vertebrate Paleontology 28 (suppl. 3): 133A-134A.

ROMANO PSR. 2010. Evolução do crânio em Pelomedusoides (Testudines, Pleurodira). D. Phil. Thesis. Museu Nacional – Universidade Federal do Rio de Janeiro.

ROMANO PSR, AZEVEDO SAK. 2006. Are extant podocnemidid turtles relicts of a widespread Cretaceous ancestor? South American Journal of Herpetology 1(3):175-184. DOI: 10.2994/1808-9798(2006)1[175:AEPTRO]2.0.CO;2.

ROMANO PSR, AZEVEDO SAK. 2007. Morphometric analysis of the Upper Cretaceous brazilian side-necked turtle *Bauruemys elegans* (Suárez, 1969) (Pleurodira, Podocnemididae). Arquivos do Museu Nacional 65(4):395-402.

ROMANO PSR, GALLO V, RAMOS RRC, ANTONIOLI L. 2014. *Atolchelys lepida*, a new side-necked turtle from the Early Cretaceous of Brazil and the age of Crown-Pleurodira. Biology Letters 10: 20140290. DOI: 10.1098/rsbl.2014.0290.

ROMANO PSR, OLIVEIRA GR, AZEVEDO SAK, CAMPOS DA. 2009. Lumping the podocnemidid turtles species from Bauru Basin (Upper Cretaceous of Southeastern of Brazil) [abstract no. 38]. Gaffney Turtle Symposium Abstract Volume: 141-152.

ROMANO PSR, OLIVEIRA GR, AZEVEDO SAK, KELLNER AWA, CAMPOS DA. 2013. New information about Pelomedusoides (Testudines: Pleurodira) from the Cretaceous of Brazil. In: Brinkman D, Holroyd P, Gardner J, ed. *Morphology and evolution of turtles.* Vertebrate Paleobiology and Paleoanthropology Series. Dordrecht, The Netherlands: Springer, 261-275.

907 SÁNCHEZ-VILLAGRA MR, AGUILERA OA. 2006. Neogene Vertebrates from Urumaco,
908 Falcón State, Venezuela: Diversity and Significance. Journal of Systematic Palaeontology
909 4(3):213-220. DOI: 10.1017/S1477201906001829.

910 SÁNCHEZ-VILLAGRA MR, WINKLER JD. 2006. Cranial variation in *Bairdemys* turtles
911 (Podocnemididae: Miocene of the Caribbean region) and description of new material from
912 Urumaco, Venezuela. Journal of Systematic Paleontology 4(3):241-253. DOI:
913 10.1017/S1477201906001891.

914 SCHUMACHER GH. 1973. The head muscles and hyolaryngeal skeleton of turtles and
915 crocodilians. In: Gans C, *Biology of Reptilia, vol. 4: Morphology D*. London: Academic Press,
916 101-199.

917 SHINE RS, IVERSON JB. 1995. Patterns of survival, growth and maturation in turtles. Oikos
918 72(3):343-348. DOI: 10.2307/3546119.

919 SMITH KK. 1993. The form of the feeding apparatus in terrestrial vertebrates: studies of
920 adaptation and constraint. In: Hanken J, Hall BK, *The Skull, Vol. 3:Functional and Evolutionary*
921 *Mechanisms.* Chicago: The University of Chicago Press, 150-196.

922 SOARES PC, LANDIM PMB, FULFARO VJ, NETO AFS. 1980. Ensaio de caracterização
923 estratigráfica do Cretáceo no estado de São Paulo: Grupo Bauru. Revista Brasileira de
924 Geociências 10:177-185.

925 SOMERS KM. 1989. Allometry, Isometry and Shape in Principal Components Analysis.
926 Systematic Zoology 38(2):169-173.

927 STERLI J, DE LA FUENTE MS. 2010. Anatomy of *Condorchelys antiqua* Sterli, 2008, and the
928 origin of the modern jaw closure mechanism in turtles. Journal of Vertebrate Paleontology
929 30(2):351-366. DOI: 10.1080/02724631003617597.

930 STERLI J, MÜLLER J, ANQUETIN J, HILGER A. 2010. The parabasisphenoid complex in
931 Mesozoic turtles and the evolution of the testudinate basicranium. Canadian Journal of Earth
932 Sciences 47:1337-1346. DOI: 10.2307/3546119.

933 STRAUSS RE, ATANASSOV MN, OLIVEIRA JA. 2003. Evaluation of the principal-
934 component and expectation-maximization methods for estimating missing data in morphometric
935 studies. Journal of Vertebrate Paleontology 23(2): 284-296.

936 SUÁREZ, JM. 1969a. Um nôvo quelônio fóssil da Formação Baurú [abstract no. 153].
937 Comunicações do Congresso Brasileiro de Geologia, Salvador: Boletim Especial, Salvador,
938 1:87-89.

939 SUÁREZ, JM. 1969b. Um quelônio da Formação Bauru. Boletim da Faculdade de Filosofia,
940 Ciências e Letras de Presidente Prudente 2:35-54.

SUÁREZ, JM. 1969c. Um quelônio da Formação Bauru [abstract no. 12]. Anais do Congresso Brasileiro de Geologia, Salvador. 167-176.

SUÁREZ JM. 2002. Sítio fossilífero de Pirapozinho, SP – Extraordinário depósito de quelônios do Cretáceo. In: Schobbenhaus C, Campos DA, Queiroz ET, Winge M, Berbert-Born M. *Sítio geológicos e paleontológicos do Brasil*.

VAN DAMME J, AERTS P. 1997. Kinematics and functional morphology of aquatic feeding in australian snake-necked turtles (Pleurodira; *Chelodina*). Journal of Morphology 233:113-125. DOI: 10.1002/(SICI)1097-4687(199708)233:2<127::AID-JMOR4>3.0.CO;2-3.

WERNEBURG I. 2011. The cranial musculature of turtles. Palaentologia eletronica 14(2):99p; palaeo-electronica.org/2011_2/254/index.html.

WERNEBURG I. 2012. Temporal bone arrangements in turtles: an overview. Journal of Experimental Zoology 318:235-249. DOI: 10.1002/jez.b.22450.

WERNEBURG I. 2013. The tendinous framework in the temporal skull region of turtles and considerations about its morphological implications in amniotes: a review. Zoological Science 30:141-153. DOI: 10.2108/zsj.30.141.

WERNEBURG I, WILSON LAB, PARR WCH, JOYCE WG. 2014. Evolution of neck vertebral shape and neck retraction at the transition to Modern Turtles: an integrated geometric morphometric approach. Systematic Biology 0(0): 1-18. DOI: 10.1093/sysbio/syu072.

WINGS O, RABI M, SCHNEIDER JW, SCHWERMANN L, SUN G, ZHOU CF, JOYCE WG. 2012. An enormous Jurassic turtle bone bed from the Turpan Basin of Xinjiang, China. Naturwissenschaften 99:925-935. DOI: 10.1007/s00114-012-0974-5.

Figure 1

Fossil turtle localities in Bauru Basin

Lithostratigraphical map of the oriental part of the Bauru Basin showing the fossil turtle localities (municipalities). Turtle species are: 1. *Cambaremys langertoni* (*incertae sedis*), *Pricemys caieira, Peiropemys mezzalirai* and Testudines indet. (Oliveira & Romano, 2007; Romano et al., 2009; Gaffney et al., 2011; Menegazzo, Bertini & Manzini, 2015); 2. *Roxochelys harrisi* (*nomem dubium*; Oliveira & Romano, 2007; Romano et al., 2009; Menegazzo, Bertini & Manzini, 2015); 3. *Bauruemys brasiliensis* (*nomem dubium*) and Testudines indet. (Oliveira & Romano, 2007; Menegazzo, 2009; Romano et al., 2009; Menegazzo, Bertini & Manzini, 2015); 4. Testudines indet. (Menegazzo, 2009; Romano et al., 2009); 5. Testudines indet. (Menegazzo, 2009; Romano et al., 2009); 6. *B. brasiliensis* and *Roxochelys wanderleyi* (Oliveira & Romano, 2007; Romano et al., 2009); **7.** Testudines indet. (Menegazzo, 2009; Romano et al., 2009); 8. Testudines indet. (Menegazzo, 2009; Romano et al., 2009); 9. Podocnemididae indet. and Testudines indet. (Menegazzo, 2009; Romano et al., 2009; Kischlat, 2015); 10. *Roxochelys* sp., *R. wanderleyi* and Testudines indet. (Menegazzo, 2009; Romano et al., 2009; Romano et al., 2013; Menegazzo, Bertini & Manzini, 2015); 11. *B. elegans* and *R. wanderleyi* (Oliveira & Romano, 2007; Romano et al., 2009; Menegazzo, Bertini & Manzini, 2015); 12. Podocnemidinura indet. (Menegazzo, Bertini & Manzini, 2015); 13. Podocnemidoiae indet. and Testudines indet. (Menegazzo, 2009; Hermanson, Ferreira & Langer, 2016); 14. *R. wanderleyi*, *B. brasiliensis* (*nomem dubium*) and Testudines indet. (Menegazzo, 2009); 15. Testudines indet. (Menegazzo, 2009); **16.** Testudines indet. (Menegazzo, 2009). **Abbreviations:** GO, Goiás State; MG, Minas Gerais State; MS, Mato Grosso do Sul State; PR, Paraná State; SP, São Paulo State. Scale bar in Km. Map modified from Romano et al. (2009); geology following Fernandes (2004); taxonomy status of species following Romano et al. (2013).

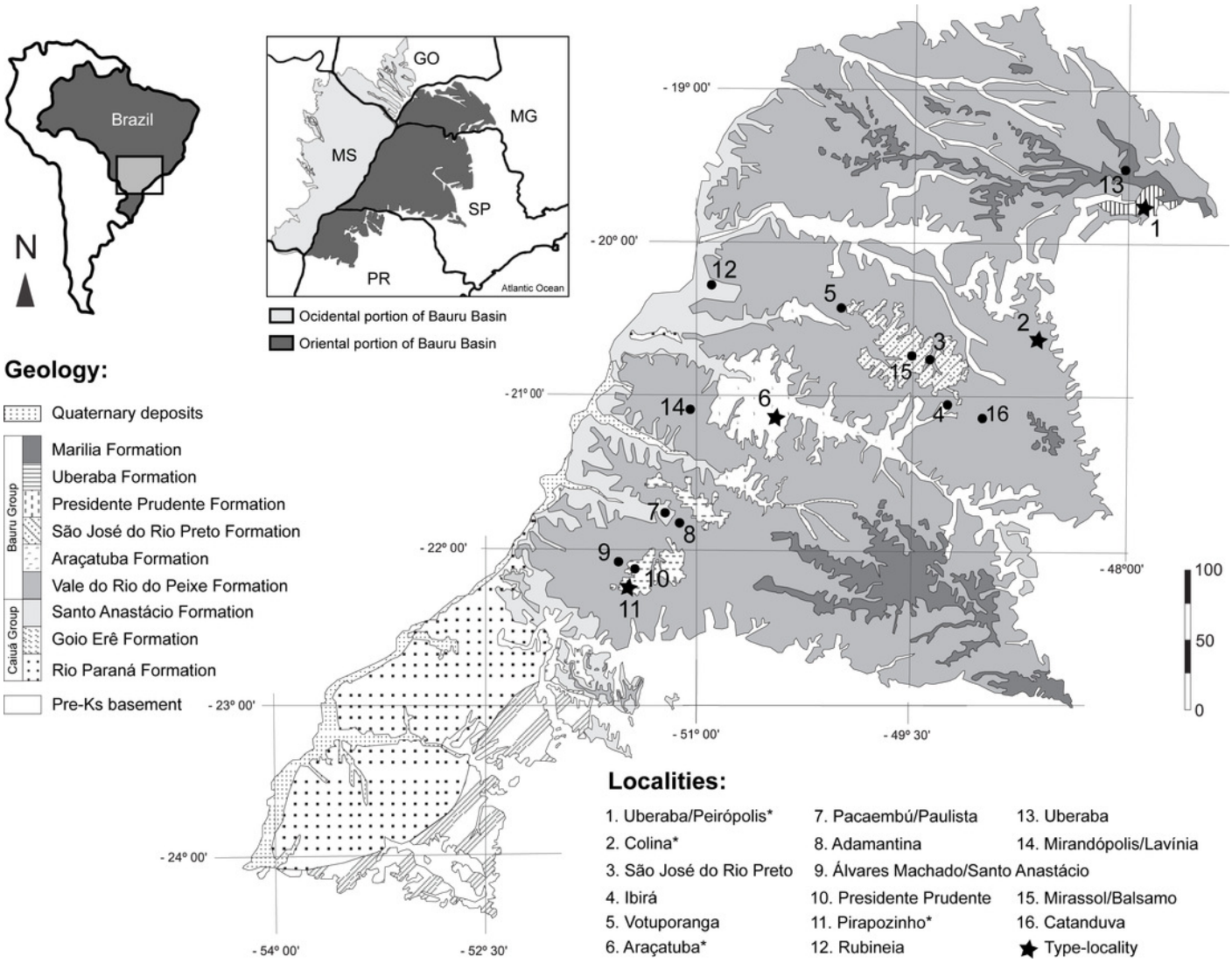
Brazil
N
GO
MG
MS
SP
PR
Atlantic Ocean
Ocidental portion of Bauru Basin
Oriental portion of Bauru Basin
Geology:
Quaternary deposits
Bauru Group
Marilia Formation
Uberaba Formation
Presidente Prudente Formation
São José do Rio Preto Formation
Araçatuba Formation
Vale do Rio do Peixe Formation
Caiuá Group
Santo Anastácio Formation
Goio Erê Formation
Rio Paraná Formation
Pre-Ks basement
- 19° 00'
- 20° 00'
- 21° 00'
- 22° 00'
- 23° 00'
- 24° 00'
- 54° 00'
- 52° 30'
- 51° 00'
- 49° 30'
- 48°00'
100
50
0
Localities:
1. Uberaba/Peirópolis*
2. Colina*
3. São José do Rio Preto
4. Ibirá
5. Votuporanga
6. Araçatuba*
7. Pacaembú/Paulista
8. Adamantina
9. Álvares Machado/Santo Anastácio
10. Presidente Prudente
11. Pirapozinho*
12. Rubineia
13. Uberaba
14. Mirandópolis/Lavínia
15. Mirassol/Balsamo
16. Catanduva
Type-locality

Figure 2

Image of landmarks used as references for taking measurements.

Skull of *Bauruemys elegans* in (A) dorsal, (B) ventral and (C) right lateral views showing the anatomical nomenclature and the 39 landmarks used for morphometrics analysis. All measurements were taken between two landmarks (see table 2 for vectors description). **Abbreviations: bo,** basioccipital; **bs,** basisphenoid; **ex,** exoccipital; **fpp,** foramen palatinum posterius; **fr,** frontal; **ju,** jugal; **mx,** maxilla; **op,** opisthotic; **pa,** parietal; **pal,** palatine; **pf,** prefrontal; **pm,** premaxilla; **po,** postorbital; **pt,** pterygoid; **ptp,** processus trochlearis pterygoidei; **qj,** quadratojugal; **qu,** quadrate; **sq,** squamosal; **so,** supraoccipital; **vo,** vomer. Skull lineation from Gaffney et al. (2011, p.72).

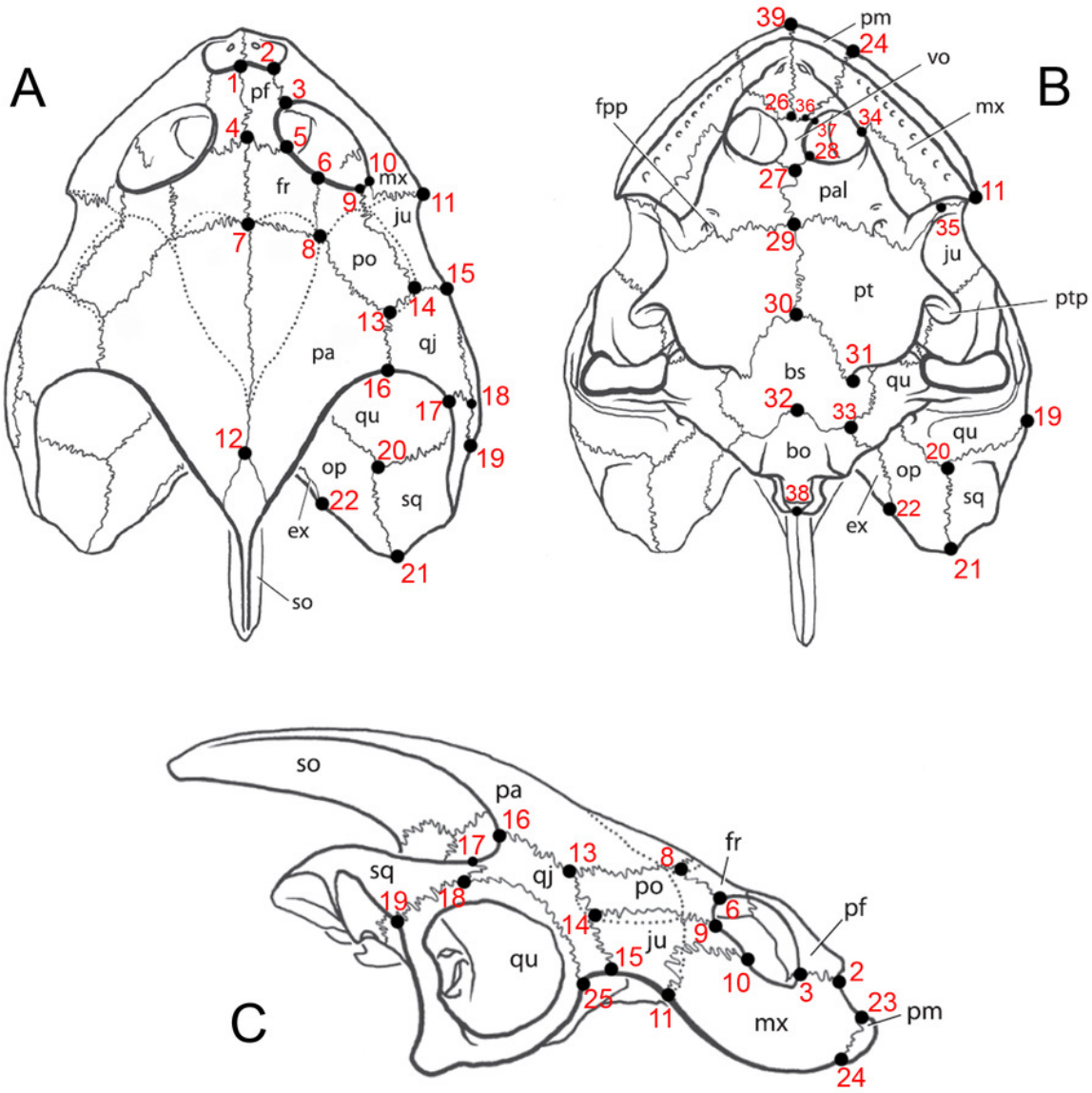
A
1
2
3
4
5
6
7
8
9
10
11
12
13
14
15
16
17
18
19
20
21
22
pf
fr
mx
ju
po
pa
qj
qu
op
sq
ex
so
B
39
pm
24
vo
fpp
26
36
37
34
mx
28
27
pal
11
29
35
ju
pt
ptp
30
31
bs
qu
32
33
19
bo
qu
20
op
38
sq
ex
22
21
C
so
pa
16
17
13
8
fr
sq
qj
po
19
18
14
6
pf
ju
9
qu
15
10
2
25
3
23
pm
11
mx
24

Figure 3

Allometric graphics: part 1.

Allometries of *Bauruemys elegans* skull bones: (A) length of parietal (LPA), (B) length of maxilla (LMX), (C), length of jugal (LJU), (D) length of quadrate (LQU), (E) length of squamosal (LSQ), (F) length of pterygoid (LPT), (G) length of postorbital (LPO), (H) stretch of maxilla (SMX), (I) width of quadratojugal (WQJ) (J) and width of parietal (WPA). Angular coefficient (a) and coefficient of correlation (r) are shown. **Abbreviations: TLS,** total length of the skull; **TWS,** total width of the skull.

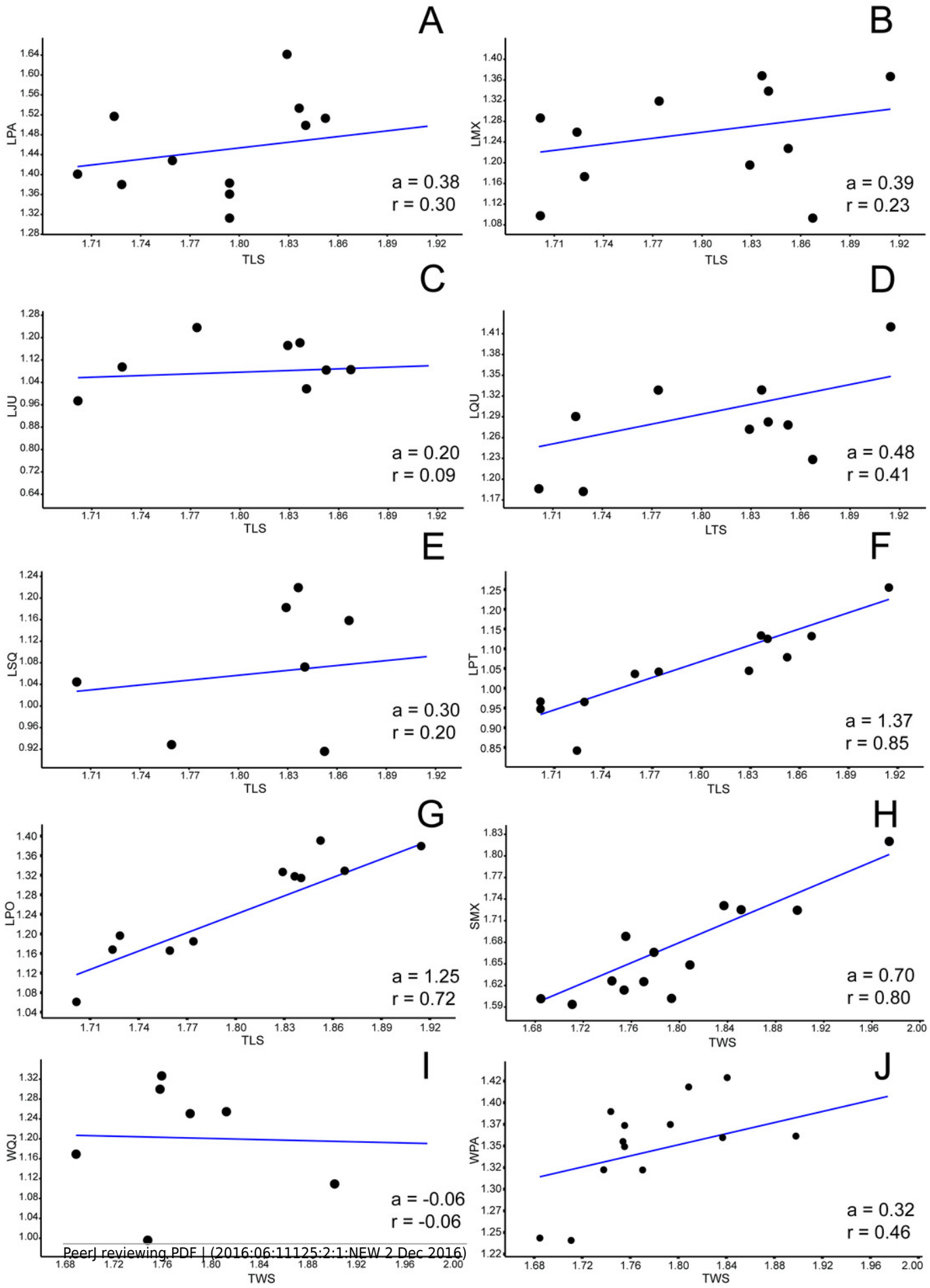
A
LPA
TLS
a = 0.38
r = 0.30
B
LMX
TLS
a = 0.39
r = 0.23
C
LJU
TLS
a = 0.20
r = 0.09
D
LQU
LTS
a = 0.48
r = 0.41
E
LSQ
TLS
a = 0.30
r = 0.20
F
LPT
TLS
a = 1.37
r = 0.85
G
LPO
TLS
a = 1.25
r = 0.72
H
SMX
TWS
a = 0.70
r = 0.80
I
WQJ
TWS
a = -0.06
r = -0.06
J
WPA
TWS
a = 0.32
r = 0.46

Figure 4

Allometric graphics: part 2.

Allometries of *Bauruemys elegans* skull bones: (A) length of basioccipital (LBO), (B) length of basisphenoid (LBS), (C), length of palatine (LPAL), (D) length of frontal (LFR), (E) length of prefrontal (LPF), (F) length of quadratojugal (LQJ), (G) length of vomer (LVO), (H) width of postorbital (WPO), (I) width of opisthotic (WOP) (J) and width of choanal (WCO). Angular coefficient (a) and coefficient of correlation (r) are shown. **Abbreviations: TLS,** total length of the skull; **TWS,** total width of the skull.

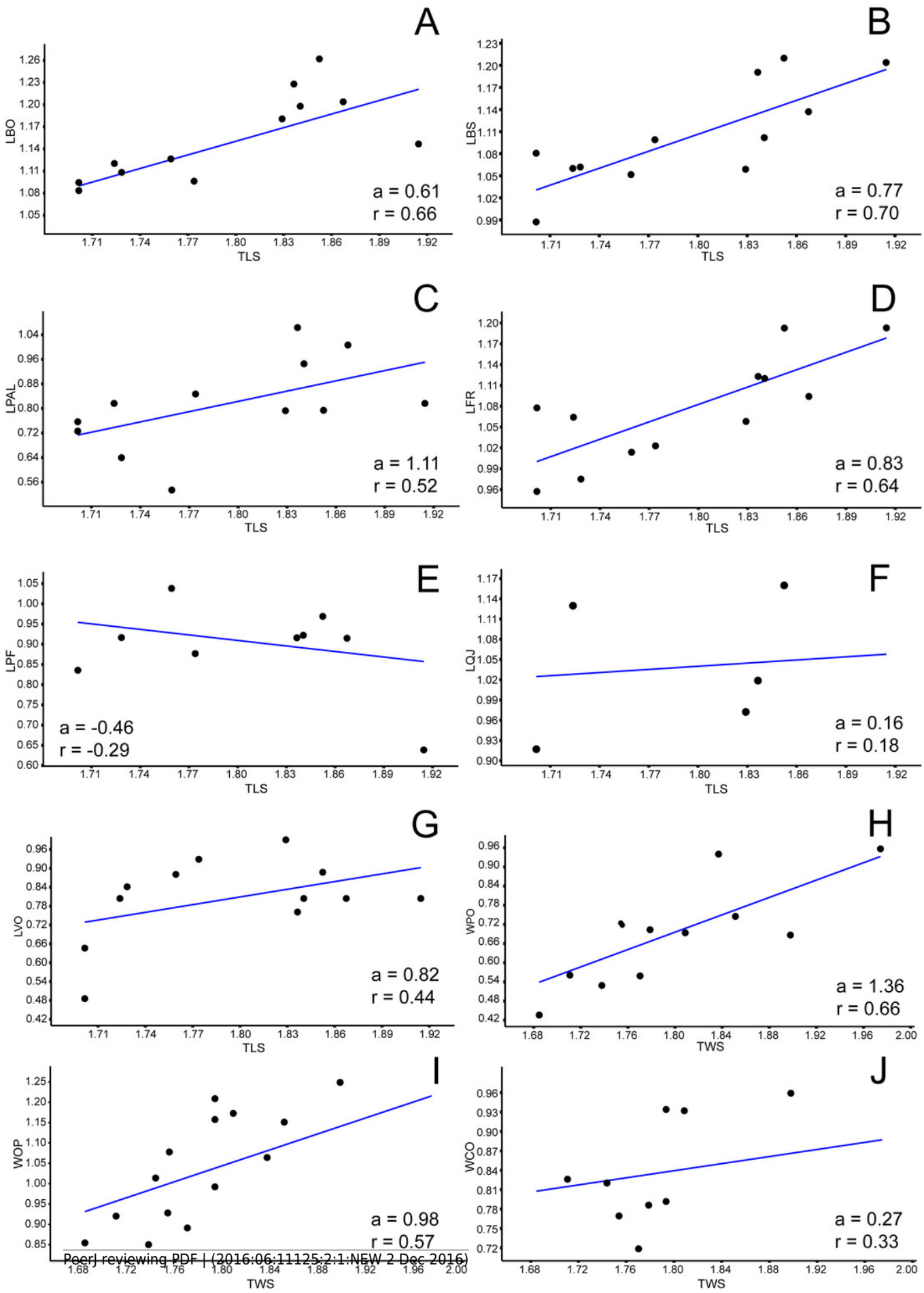
A
LBO
TLS
a = 0.61
r = 0.66
B
LBS
TLS
a = 0.77
r = 0.70
C
LPAL
TLS
a = 1.11
r = 0.52
D
LFR
TLS
a = 0.83
r = 0.64
E
LPF
TLS
a = -0.46
r = -0.29
F
LQJ
TLS
a = 0.16
r = 0.18
G
LVO
TLS
a = 0.82
r = 0.44
H
WPO
TWS
a = 1.36
r = 0.66
I
WOP
TWS
a = 0.98
r = 0.57
J
WCO
TWS
a = 0.27
r = 0.33

Figure 5

Allometric graphics: part 3.

Allometries of *Bauruemys elegans* skull bones: (A) width of maxilla (WMX), (B) width of jugal (WJU), (C), width of frontal (WFR), (D) width of prefrontal (WPF), (E) width of basisphenoid (WBS), (F) width of palatine (WPAL) and (G) width of vomer (WVO). Angular coefficient (a) and coefficient of correlation (r) are shown. **Abbreviations: TWS,** total width of the skull.

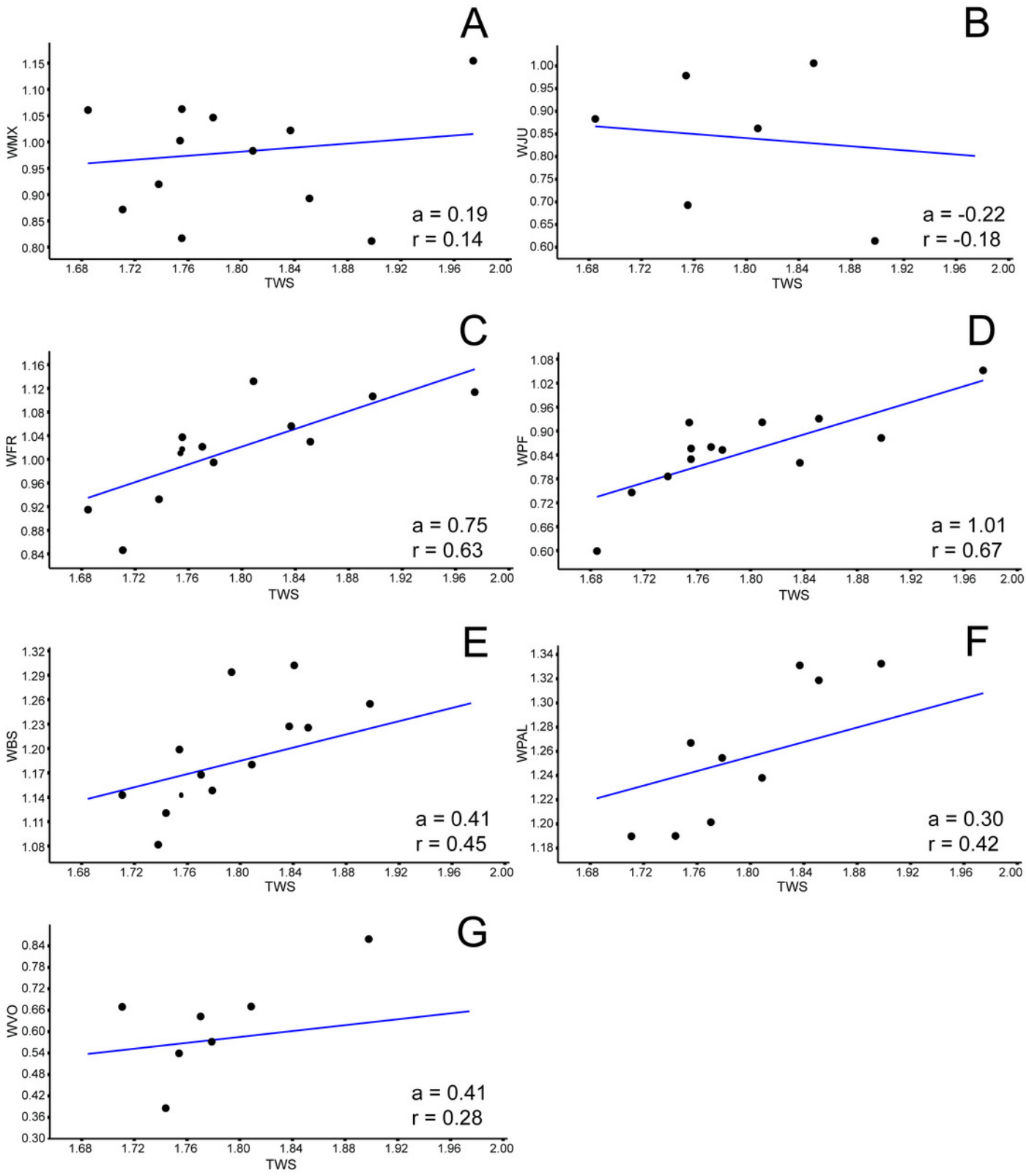
A
WMX
TWS
a = 0.19
r = 0.14
B
WJU
TWS
a = -0.22
r = -0.18
C
WFR
TWS
a = 0.75
r = 0.63
D
WPF
TWS
a = 1.01
r = 0.67
E
WBS
TWS
a = 0.41
r = 0.45
F
WPAL
TWS
a = 0.30
r = 0.42
G
WVO
TWS
a = 0.41
r = 0.28

Figure 6

PCA: raw data.

Principal Components Analysis (PCA) from raw data matrix using mean value substitution approach (A and B) and iterative imputation substitution approach (C) in replacing missing data. The 95% ellipse is given.

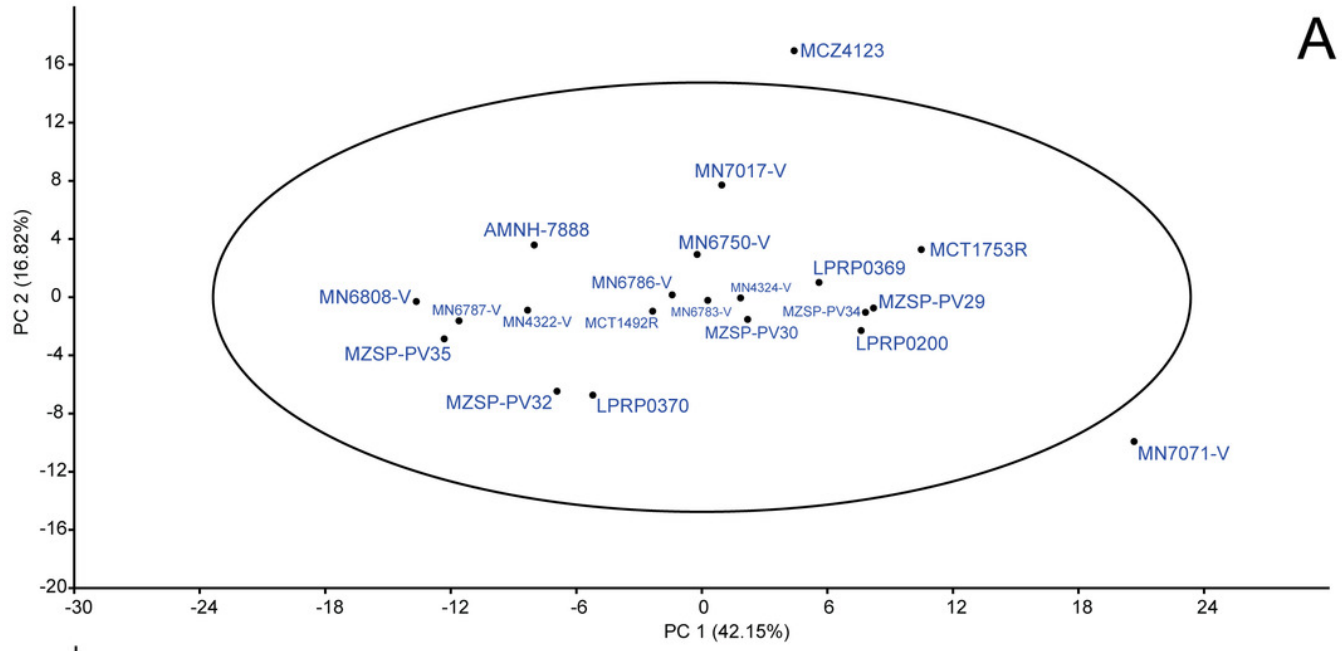
A
MCZ4123
MN7017-V
AMNH-7888
MN6750-V
MCT1753R
LPRP0369
MN6786-V
MN4324-V
MN6808-V
MN6787-V
MN4322-V
MCT1492R
MN6783-V
MZSP-PV34
MZSP-PV29
MZSP-PV30
LPRP0200
MZSP-PV35
MZSP-PV32
LPRP0370
MN7071-V
PC 2 (16.82%)
PC 1 (42.15%)

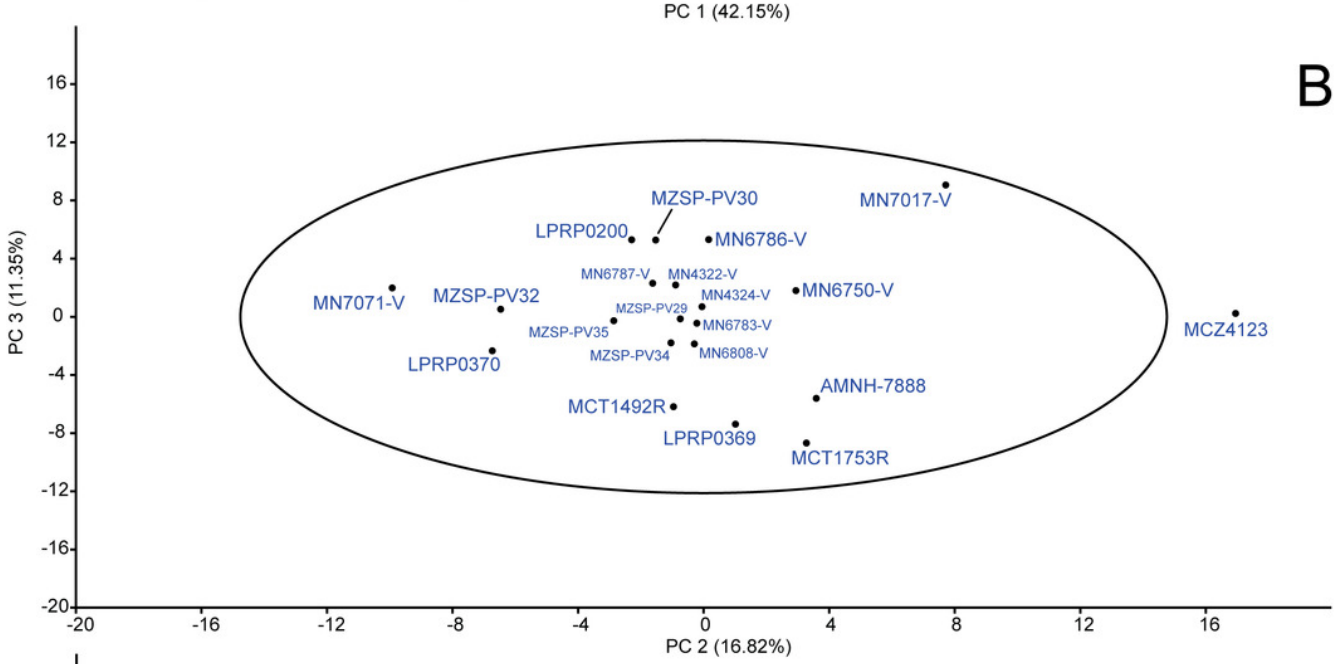
B
MZSP-PV30
MN7017-V
LPRP0200
MN6786-V
MN6787-V
MN4322-V
MN7071-V
MZSP-PV32
MN4324-V
MN6750-V
MZSP-PV29
MZSP-PV35
MN6783-V
MCZ4123
MZSP-PV34
MN6808-V
LPRP0370
AMNH-7888
MCT1492R
LPRP0369
MCT1753R
PC 3 (11.35%)
PC 2 (16.82%)

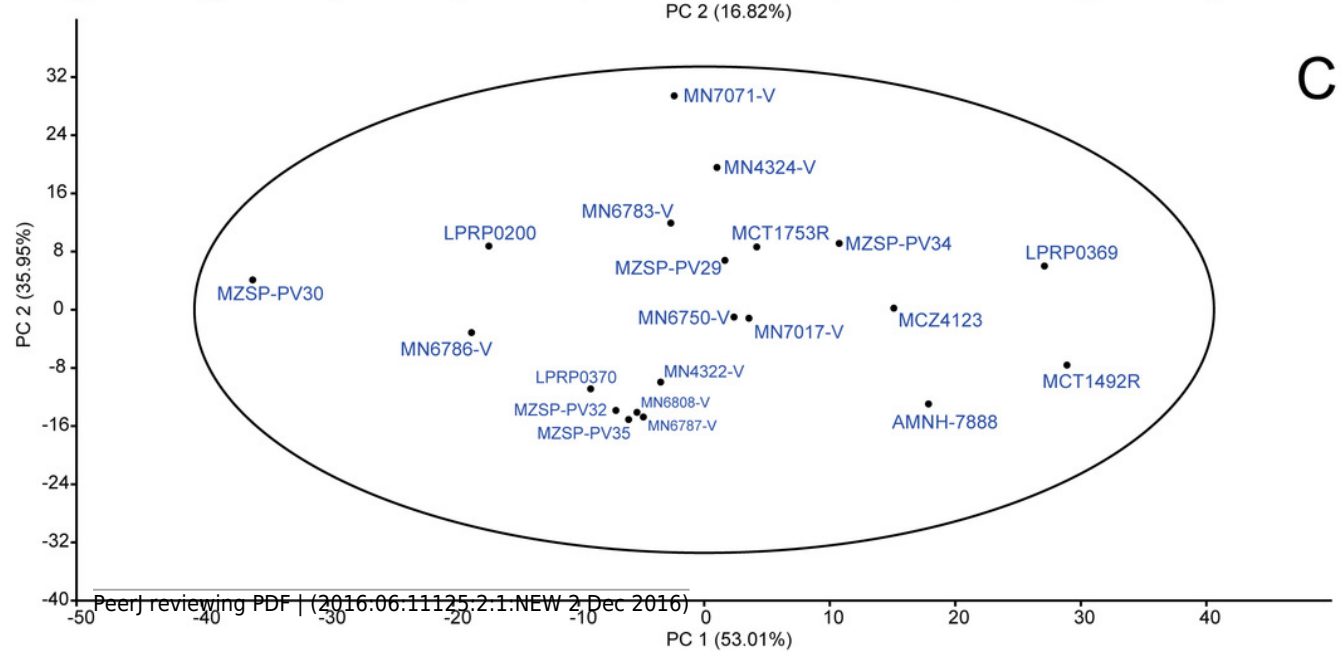
C
MN7071-V
MN4324-V
MN6783-V
LPRP0200
MCT1753R
MZSP-PV34
LPRP0369
MZSP-PV29
MZSP-PV30
MN6750-V
MN7017-V
MCZ4123
MN6786-V
LPRP0370
MN4322-V
MCT1492R
MZSP-PV32
MN6808-V
MZSP-PV35
MN6787-V
AMNH-7888
PC 2 (35.95%)
PC 1 (53.01%)

Figure 7

PCA: proportions data.

Principal Components Analysis (PCA) from proportions data matrix using mean value substitution approach (A) and iterative imputation substitution approach (B) in replacing missing data. The 95% ellipse is given.

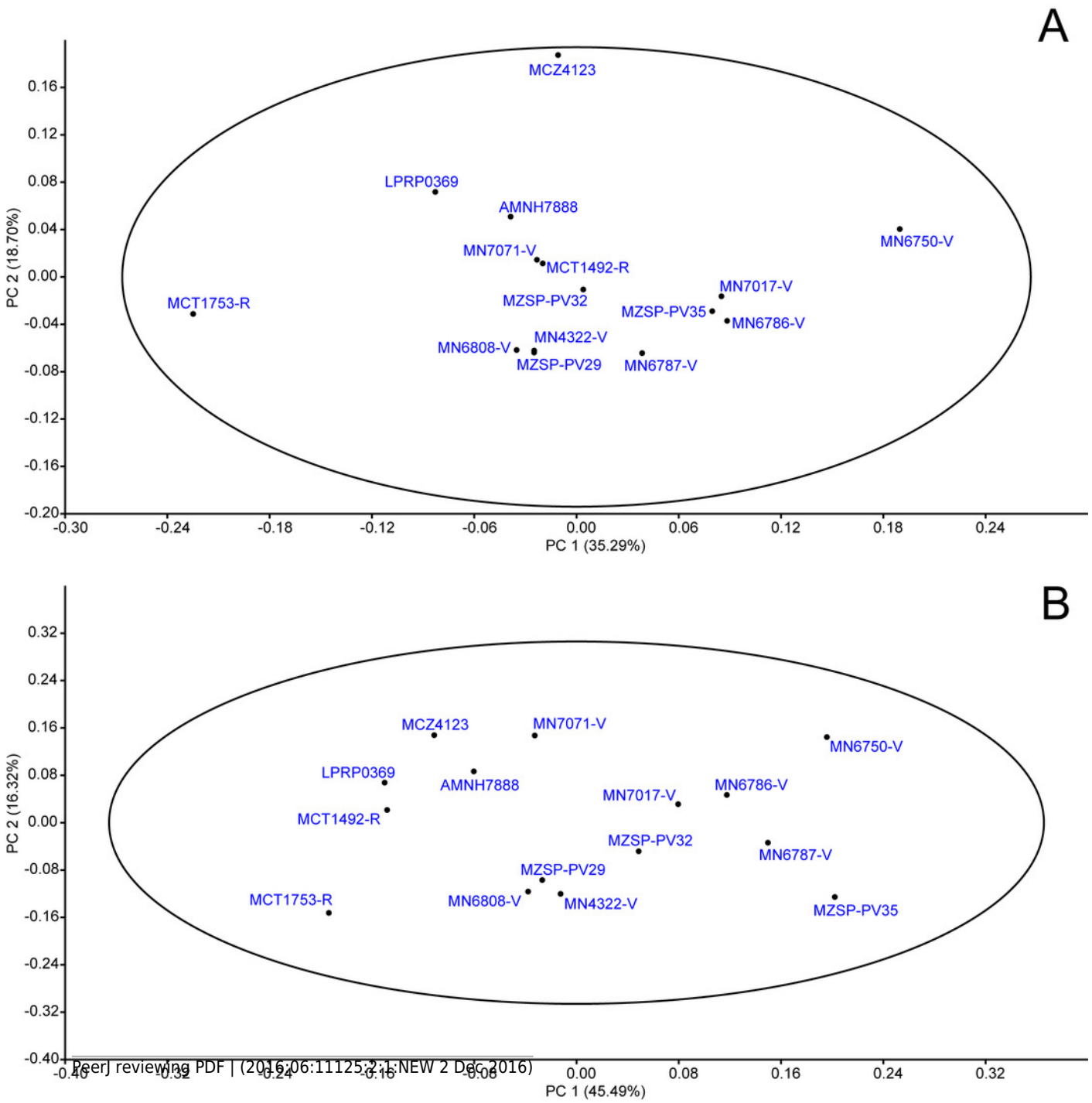

Figure 8

Comparison of a taphonomically altered skull with two well-preserved skulls of *Bauruemys elegans*, showing the cheek morphologies observed.

Bauruemys elegans specimens in dorsal view showing the largest MN7071-V specimen (A) in contrast with two smaller, well-preserved narrow-cheeked MN7017-V (B) and wide-cheeked MN4322-V (C) specimens. MN7071-V (A) is larger due to vertical crushing in the mediocaudal portion of the skull, resulting in artificial wide-cheeked morphology. In other specimens, such a taphonomic effect is not observed, indicating that both narrow- (B) and wide-cheeked (C) morphologies are naturally present in *B. elegans*.

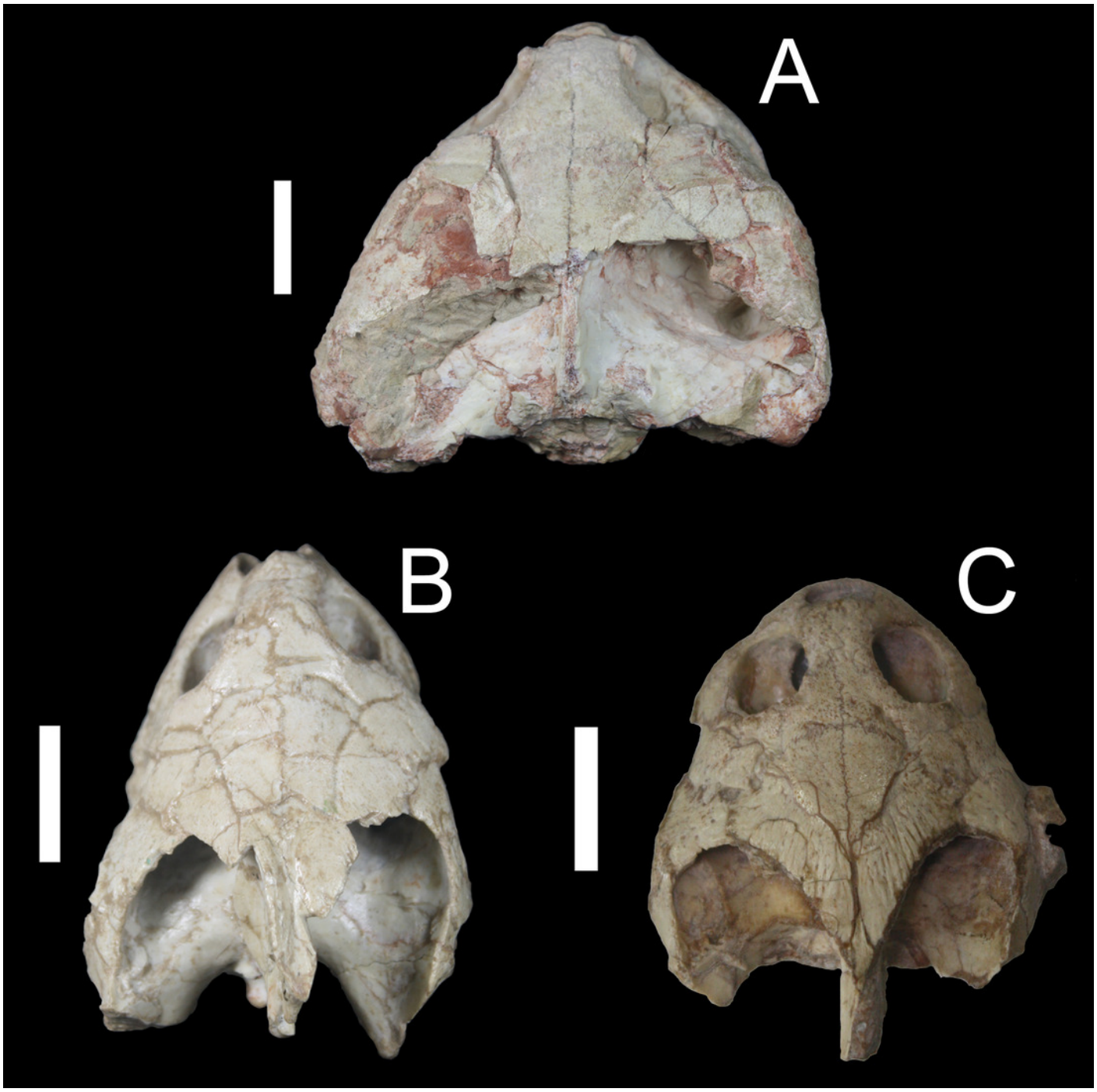
A
B
C

Figure 9

Evolution of PA-QJ contact and skull roofing in Podocnemidoidea.

Simplified phylogeny of Podocnemidoidea (Bothremydidae + Podocnemidinura) showing the evolution of the contact between parietal (green; PA) and quadratojugal (yellow; QJ), and its relation with the postorbital (red; PO) and skull roofing. Within Bothremydidae, both very emarginated (*Cearachelys placidoi*) and less emarginated (*Taphrosphys congolensis*) skulls are present, showing either no contact (*C. placidoi)* or contact present with small QJ (*T. congolensis*). Within Podocnemidinura, the contact PA-QJ is present and the skull roofing increased from a less roofed condition, found in *Brasilemys josai* and *Hamadachelys*, to a continuous increasingly growing well roofed condition within Podocnemididae, exemplified by *Bauruemys elegans*, *Lapparentemys vilavillensis* and *Podocnemis unifilis*, up to a fully roofed morphology in *Peltocephalus*. *Cearachelys placidoi* and *T. congolensis* modified from Gaffney et al. (2006); *Brasilemys josai* redrawn from Lapparent de Broin (2000); all others skulls modified from Gaffney et al. (2011).

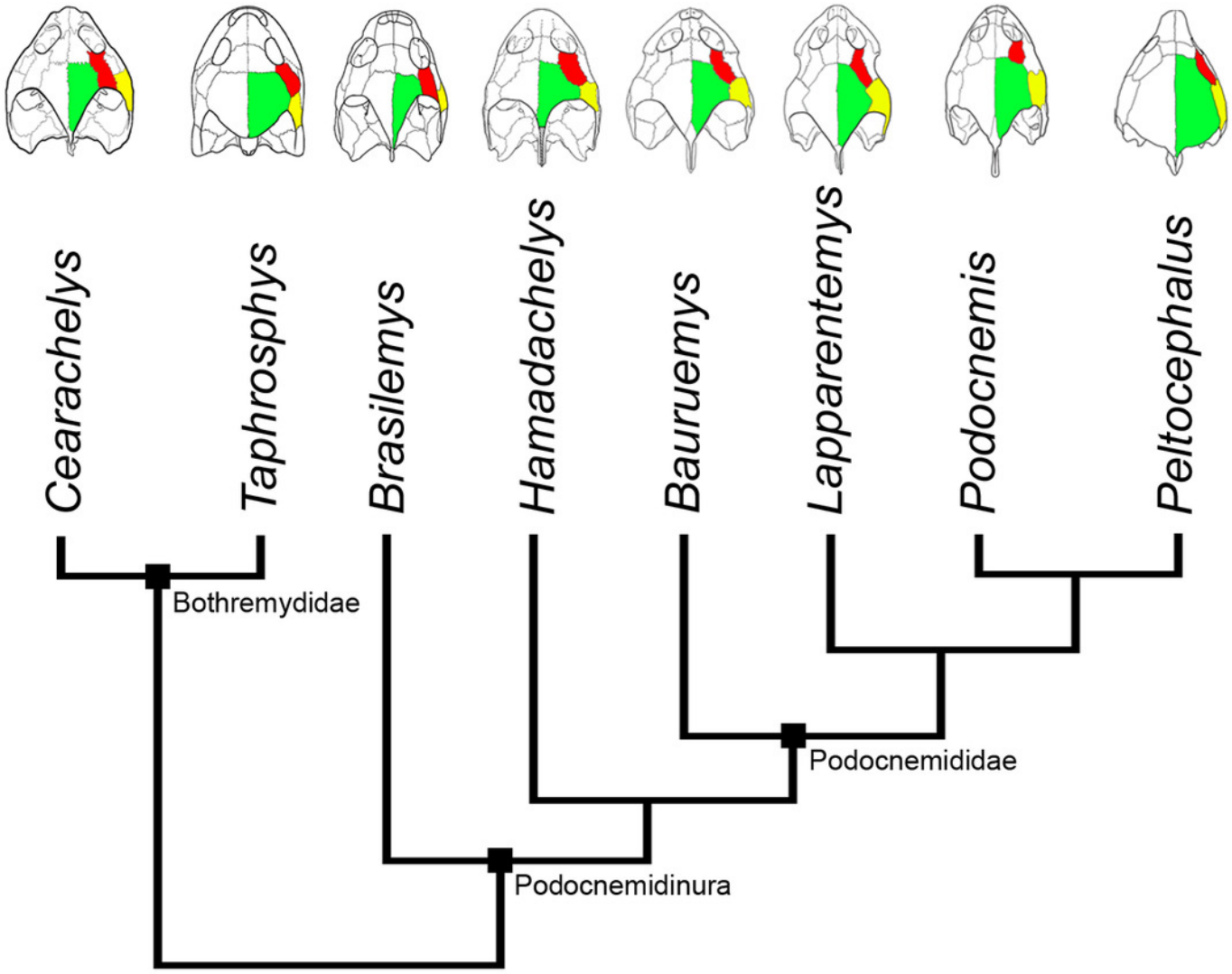
Cearachelys
Taphrosphys
Brasilemys
Hamadachelys
Bauruemys
Lapparentemys
Podocnemis
Peltocephalus
Bothremydidae
Podocnemididae
Podocnemidinura

Figure 10

Sketch of jaw-closing muscles and its vector forces in *Podocnemis expansa*.

Dorsal (A and C) and left lateral (B and D) view of the skull of *Podocnemis expansa* (MZSP-0038) showing the muscle attachment places (A and B) and the direction vector forces (C and D) during jaw closing. The muscles and vectors of *m. adductor mandibulae externus* (green), *m. adductor mandibulae posterior* (red), *m. pterygoideus* (blue), and *m. depressor mandibulae* (yellow) are sketched. Length and thickness of the arrows indicate the relative forces. **Abbreviations:** art, articular; **den,** dentary; **mx,** maxilla; **pa,** parietal; **ptp,** processus trochlearis pterygoidei; **qj,** quadratojugal; **qu,** quadrate; **so,** supraoccipital.

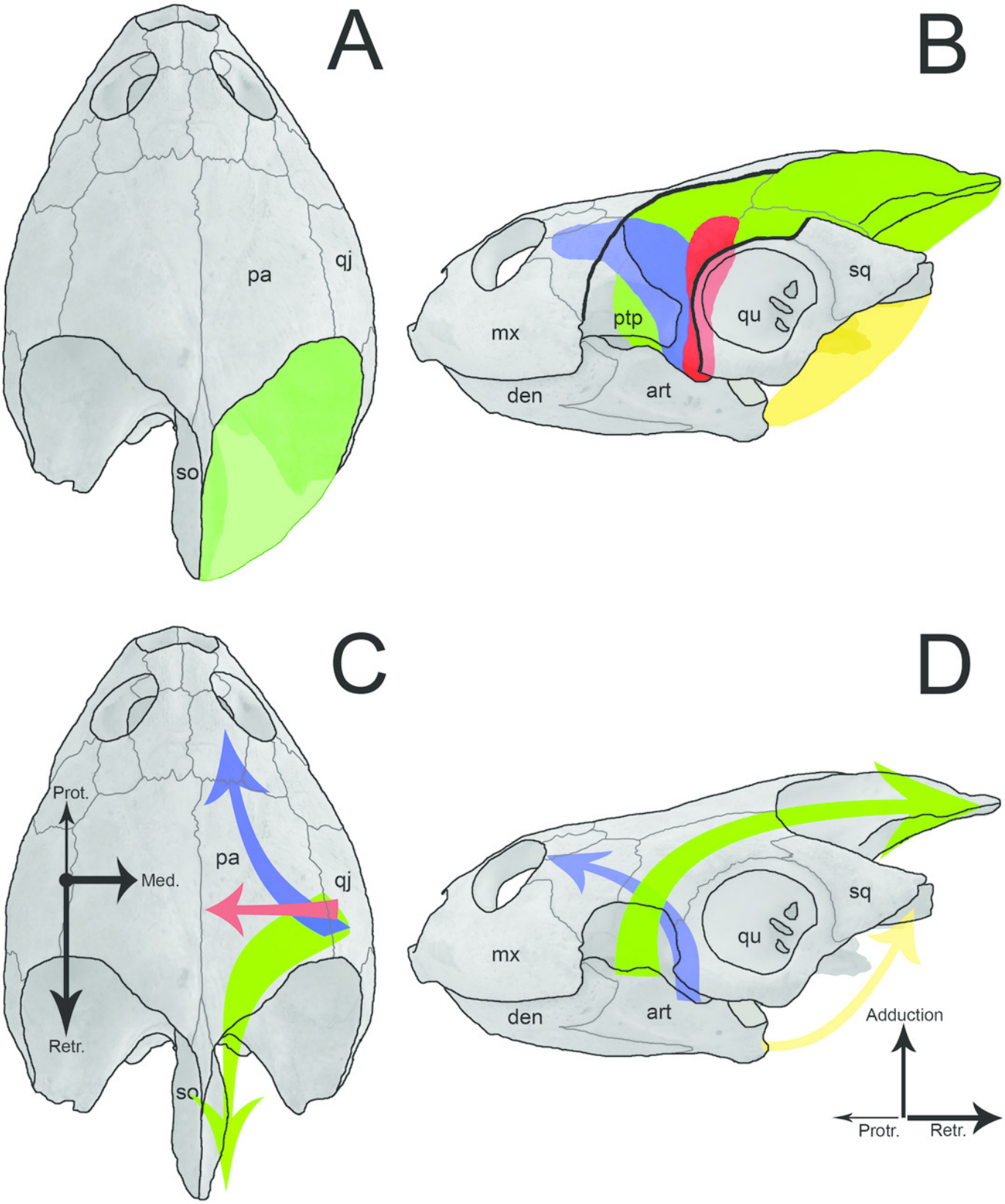
A
pa
qj
so
B
mx
ptp
qu
sq
den
art
C
Prot.
Med.
Retr.
pa
qj
so
D
mx
qu
sq
den
art
Adduction
Protr.
Retr.

Table 1(on next page)

ANOVA results for ImageJ and caliper comparisons.

Parameters calculated for each treatment of the ANOVA. Columns 2, 3, and 4 are relative to the caliper (cal) are relative to the ImageJ (ImJ). The last column indicates the F values for each character. Measurements abbreviations: TLS, total length of the skull; TWS total width of the skull; LPF, length of prefrontal; WPF, width of prefrontal; LFR, length of frontal; WFR, width of frontal; LPA, length of parietal; WPA, width of parietal; SMX, stretch of maxilla; LVO, length of vomer; WVO, width of vomer; WCO, width of choannal; LPAL, length of palatine; WPAL, width of palatine; LPT, length of pterygoid; LBS, length of basisphenoid; WBS, width of basisphenoid; LBO, length of basisoccipital; LMX, length of maxilla; WMX, width of maxilla; LJU, length of jugal; WJU, width of jugal; LQJ, length of quadratojugal; WQJ, width of quadratojugal; LQU, length of quadrate; LPO, length of postorbital; WPO, width of postorbital; WOP, width of opisthotic; LSQ, length of squamosal.

Char.	N (Cal)	Mean (Cal)	σ (Cal)	N (ImJ)	Mean (ImJ)	σ (ImJ)	F value
TLS	8	63,72	10,87	8	62,26	11,36	0,069
TWS	9	60,42	9,45	8	64,83	13,58	0,617
LPF	9	9,78	1,26	9	8,05	1,80	5,617*
WPF	10	6,70	1,90	10	7,55	1,83	1,04
LFR	10	12,19	1,74	10	11,79	2,02	0,233
WFR	10	9,64	1,63	10	10,12	1,82	0,383
LPA	7	25,54	4,71	7	27,35	4,83	0,504
WPA	6	21,78	2,79	6	22,54	3,16	0,195
SMX	9	46,46	7,12	9	47,66	8,62	0,104
LVO	6	5,95	1,71	7	6,59	1,31	0,596
WVO	6	3,11	0,78	7	3,68	0,52	1,874
WCO	5	7,53	1,31	6	6,45	1,15	2,107
LPAL	7	8,26	1,25	8	7,21	2,81	0,828
WPAL	7	16,90	1,91	7	17,12	2,23	0,038
LPT	11	11,54	2,06	12	11,69	2,75	0,228
LBS	12	12,43	1,30	12	12,88	1,64	0,563
WBS	11	15,58	2,32	11	15,57	2,40	<0,001
LBO	7	13,00	1,84	7	13,84	1,85	0,726
LMX	10	24,28	4,20	9	19,22	4,15	6,937*
WMX	10	10,44	2,16	9	10,18	2,26	0,065
LJU	9	15,75	3,81	7	13,39	2,92	1,847
WJU	3	8,31	1,20	2	9,83	-**	2,709
LQJ	4	12,84	1,48	2	11,96	-**	0,366
WQJ	6	16,21	4,02	3	19,65	1,72	1,921
LQU	11	17,71	3,43	8	21,19	3,88	4,253
LPO	9	16,57	3,30	9	16,89	4,11	0,35
WPO	9	5,47	1,77	8	5,44	1,73	0,002
WOP	6	11,97	2,52	5	10,98	3,89	0,260
LSQ	5	10,63	3,28	4	12,26	3,86	0,467

1 Cal: caliper treatment. ImJ: ImageJ treatment. *significant statistically differences. **values not
2 calculated.

Table 2(on next page)

Descriptive statistics of all data.

Descriptive statistics of the three sorts of characters analyzed (total length and width, comprised measurements, and proportions of the measurements), including mean values (Mean), median values (Median), standard deviation values (SD), number of entries (N), and maximum and minimum values (Max-Min). All measurements are expressed in millimeters, except unscaled proportions between two measurements.

	Characters	Vector[a]	N	Mean	Median	SD	Min-Max
Total Length and Width	**TLS**	38-39	12	63.02	63.44	10.43	50.3-82.15
	TWS	-	15	63.08	58.93	11.91	48.39-94.27
Comprised measurements	**LPF**	1-4	15	8.35	8.31	1.69	4.35-10.94
	LFR	4-7	18	12.16	12.32	2.08	9.06-15.59
	LPA	7-12	12	28.88	27.36	6.45	20.54-43.80
	LVO	26-27	10	6.67	6.84	1.95	3.06-9.79
	LPAL	27-29	13	6.91	6.22	2.33	3.42-11.57
	LPT	29-30	19	11.72	11.94	2.42	6.95-17.99
	LBS	30-32	20	12.76	12.57	1.77	9.71-16.21
	LBO	32-38	13	14.16	13.38	2.12	11.13-18.28
	LMX	11-24	18	18.49	18.31	4.11	12.39-25.68
	LJU	10-14	14	12.42	12.32	3.28	4.46-17.22
	LQJ	13-18	6	11.15	10.66	2.38	8.26-14.45
	LQU	19-25	14	19.83	19.35	3.51	15.21-26.30
	LPO	6-13	17	17.54	15.72	4.12	11.51-24.59
	LSQ	20-21	11	11.71	11.08	3.07	8.24-16.57
	WPF	4-5	18	7.17	7.15	1.66	3.97-11.27
	WFR	7-8	18	10.55	10.61	1.88	7.02-13.55
	WPA	12-16	12	22.53	22.94	2.94	17.41-26.85
	SMX	11-11	15	47.85	46.35	7.63	39.24-66.10
	WVO	28-28	10	4.01	3.74	1.38	2.43-7.23
	WCO	28-34	9	7.00	6.61	1.39	5.23-9.10
	WPAL	29-35	14	18.08	18.23	2.37	15.24-21.50

	WBS	33-33	19	15.35	14.71	2.19	12.07-20.05
	WMX	10-11	16	9.80	9.84	2.24	6.48-14.27
	WJU	14-15	7	7.26	7.28	2.19	4.11-10.14
	WQJ	16-25	7	16.35	17.81	4.03	9.91-21.21
	WPO	13-14	16	5.15	5.00	1.83	2.73-9.05
	WOP	20-22	14	11.41	10.96	3.54	7.78-17.73
	CHARACTERS	**N**	**MEAN**		**MEDIAN**	**SD**	**MIN-MAX**
PROPORTIONS OF THE MEASUREMENTS	**LPF/TLS**	9	0.13		0.13	0.04	0.05-0.19
	LFR/TLS	11	0.19		0.18	0.02	0.17-0.22
	LPA/TLS	8	0.51		0.49	0.08	0.45-0.65
	LVO/TLS	8	0.11		0.12	0.03	0.06-0.15
	LPAL/TLS	10	0.11		0.11	0.03	0.06-0.17
	LPT/TLS	12	0.18		0.18	0.02	0.13-0.22
	LBS/TLS	12	0.21		0.21	0.02	0.17-0.24
	LBO/TLS	11	0.24		0.24	0.02	0.21-0.26
	LMX/TLS	11	0.29		0.28	0.06	0.17-0.38
	LJU/TLS	8	0.21		0.21	0.05	0.15-0.29
	LQJ/TLS	5	0.18		0.16	0.05	0.14-0.25
	LQU/TLS	10	0.30		0.30	0.04	0.23-0.37
	LPO/TLS	11	0.29		0.29	0.03	0.23-0.35
	LSQ/TLS	7	0.19		0.20	0.05	0.12-0.24
	WPF/TWS	13	0.12		0.12	0.02	0.08-0.15
	WFR/TWS	13	0.17		0.17	0.02	0.14-0.21
	WPA/TWS	10	0.37		0.37	0.05	0.29-0.44

SMX/TWS	12	0.75	0.76	0.06	0.67-0.86
WVO/TWS	7	0.09	0.07	0.02	0.04-0.09
WCO/TWS	7	0.11	0.12	0.02	0.09-0.13
WPAL/TWS	9	0.29	0.29	0.02	0.27-0.32
WBS/TWS	12	0.24	0.24	0.02	0.22-0.28
WMX/TWS	12	0.16	0.15	0.04	0.08-0.24
WJU/TWS	6	0.12	0.13	0.05	0.05-0.17
WQJ/TWS	7	0.29	0.30	0.08	0.16-0.37
WPO/TWS	12	0.08	0.08	0.02	0.06-0.13
WOP/TWS	11	0.18	0.17	0.04	0.13-0.23

SD: standard deviation values. N: number of entries. Max-Min: maximum and minimum values.
[a] straight line between two landmarks used to trace linear measurements (see figure 2 to visualize the landmarks).

Table 3(on next page)

PCA loadings: raw data.

Loading values of characters in the raw data matrix related to the first three principal components in PCA, comparing the Mean Value (mv) approach with the Iterative Imputation (ii) approach.

Char.	PC1 (mv)	PC2 (mv)	PC3 (mv)	PC1 (ii)	PC2 (ii)	PC3 (ii)
LPF	-0.05	0.04	0.02	-0.04	-0.05	-0.05
WPF	0.14	0.02	0.05	-0.001	0.12	0.08
LFR	0.19	-0.01	-0.09	0.02	0.14	-0.04
WFR	0.17	0.10	-0.02	0.01	0.13	-0.001
LPA	0.27	0.74	0.10	0.89	0.04	0.11
WPA	0.12	0.17	-0.01	0.22	0.16	0.06
SMX	0.66	-0.45	-0.22	0.01	0.59	-0.34
LVO	0.05	0.07	0.03	-0.02	0.11	0.01
WVO	0.04	0.03	-0.07	0.02	0.09	-0.11
WCO	0.05	0.04	-0.07	0.03	0.12	-0.08
LPAL	0.08	0.04	0.06	0.04	0.13	0.27
WPAL	0.15	0.02	-0.09	0.03	0.23	-0.05
LPT	0.17	-0.14	0.08	-0.02	0.13	0.10
LBS	0.14	-0.02	0.01	0.01	0.10	0.05
WBS	0.12	0.05	-0.07	0.02	0.19	-0.05
LBO	0.11	0.11	-0.07	0.03	0.20	0.03
LMX	0.18	-0.17	0.68	-0.18	0.16	0.38
WMX	0.09	-0.07	0.25	-0.08	0.11	0.19
LJU	0.08	0.13	0.30	-0.14	0.19	0.25
WJU	-0.01	0.02	0.10	0.01	-0.01	0.21
LQJ	0.04	-0.05	-0.04	-0.16	0.18	-0.11
WQJ	0.03	0.07	0.29	-0.11	0.17	0.42
LQU	0.18	-0.13	0.32	-0.13	0.21	0.18
LPO	0.36	0.19	-0.13	0.03	0.29	0.02
WPO	0.11	-0.04	0.05	-0.01	0.10	0.04
WOP	0.21	0.15	-0.23	0.06	0.30	-0.24
LSQ	0.07	0.19	0.11	0.16	0.02	0.43

1 Char: characters. mv: Mean Value approach. ii: Iterative Imputation approach.

Table 4(on next page)

PCA loadings: proportion data.

Loading values of characters in the proportions data matrix related to the first two principal components in PCA, comparing the Mean Value (mv) approach with the Iterative Imputation (ii) approach.

Char.	PC1 (mv)	PC2 (mv)	PC1 (ii)	PC2 (ii)
LPF/TLS	0.003	-0.13	0.11	-0.30
LFR/TLS	0.001	-0.04	0.03	-0.02
LPA/TLS	0.28	0.66	-0.13	0.67
LVO/TLS	-0.002	0.05	-0.03	-0.02
LPAL/TLS	0.08	0.02	0.07	0.12
LPT/TLS	-0.05	-0.10	-0.02	-0.01
LBS/TLS	0.03	-0.17	0.11	-0.10
LBO/TLS	-0.02	-0.04	0.01	-0.04
LMX/TLS	0.38	-0.43	0.48	-0.18
LJU/TLS	0.16	0.01	0.16	0.14
LQJ/TLS	0.06	-0.09	0.21	-0.17
LQU/TLS	0.27	-0.07	0.28	0.05
LPO/TLS	-0.16	0.13	-0.18	0.03
LSQ/TLS	0.16	0.23	0.20	0.34
WPF/TWS	0.07	0.09	-0.001	0.11
WFR/TWS	0.07	0.13	0.02	0.05
WPA/TWS	0.23	0.32	0.08	0.33
SMX/TWS	0.38	-0.12	0.33	-0.01
WVO/TWS	-0.05	-0.04	-0.04	-0.10
WCO/TWS	-0.04	0.07	-0.11	0.04
WPAL/TWS	0.04	-0.07	0.04	-0.003
WBS/TWS	0.03	-0.05	0.02	-0.03
WMX/TWS	0.35	-0.05	0.30	0.03
WJU/TWS	0.18	0.01	0.26	0.19
WQJ/TWS	0.48	-0.003	0.41	0.20
WPO/TWS	0.02	0.01	-0.01	0.07
WOP/TWS	-0.13	0.27	-0.21	0.09

1 Char: characters. mv: Mean Value approach. ii: Iterative Imputation approach.